Radiocommunication Study Groups

Received: 3 October 2022

Document 5D/1533-E
5 October 2022
English only

SPECTRUM ASPECTS &
WRC-23 PREPARATIONS

France

DYNAMIC STUDY BETWEEN RADIOLOCATION AND IMT OPERATING IN 10 000- 10 500 MHz UNDER AGENDA ITEM 1.2

1 Introduction

During the previous meeting of Working Party (WP) 5D, several contributions updated sharing and compatibility studies between radiolocation and IMT systems operating in the 10 000-10 500 MHz frequency band in Region 2. The outcome is available in the working document from Chairman's report (see Chapter 4 Annex 4.22).

2 Discussion

The study previously submitted by France (Doc. 5D/1141) addressed the protection of the airborne radar in a **fixed position** when **pointing to a specific direction** (IMT network) as suggested by WP 5B previous LS (see Document 5D/1007) quoting, among others *for aggregated scenarios, WP 5B proposes WP 5D to take into account the interference received by the radar only when pointing in the direction of the IMT deployment*. Under such assumptions, that analysis could be considered as a static analysis.

During the previous meeting, it was observed that such scenario might not be realistic as it is related to a specific case where the aircraft is pointing to the specific direction of the sources of interference under propagation conditions that may maximize the aggregate interference compared to practical situations. In addition, it was further noted that when conducting dynamic simulations for sharing and compatibility studies, the interference received by the radar from IMT deployment should be considered "*using the complete radar antenna pattern with its recommended antenna scanning parameters is required*" (***5D/1183***). France explained that the guidance from WP5B sought at protecting any radiolocation system at every angular direction, in particular those which would suffer from higher aggregate interference level. The same administration expressed no difficulty to consider the operational usage of the airborne radar with rotating antenna (i.e. with main lobe, side lobes and back-lobes pointing towards the IMT network) from the moment the scanning angles are not combined when computing the aggregate interference and sufficient number of samples is generated in Monte-Carlo simulations.

From these observations, France undertook a dynamic study with an aircraft in mobility flying outside territories under the jurisdiction of any administration for which radar antenna azimuth and elevation scanning are considered. The impact of IMT Base Stations over the airborne receiver during its operation is further investigated.

3 Proposal

In light of numerous different assumptions driving this analysis, this document proposes a new Study G to the Attachment of the working document on sharing and compatibility studies of IMT systems in the frequency band 10 000-10 500 MHz.

Attachment: 1

ATTACHMENT

Sharing and compatibility of the Radiolocation and IMT operating in the frequency band 10 000-10 500 MHz

2.7 Study G

2.7 Technical characteristics

2.7.1 Technical and operational characteristics of IMT systems operating in the frequency band 10 000 - 10 500 MHz

2.7.1.1 Technical characteristics

2.7.1.1.1 AAS beamforming characteristics

Document 5D/716 Annex 4.4 of the Chairman's Report provides the characteristics of the AAS antenna to be used in conjunction with the radiation pattern given in Recommendation ITU-R M.2101-0 (Annex 1 section 5) when generating emissions levels of the IMT base stations.

TABLE 1

Beamforming antenna characteristics for IMT in 6 425-10 500 MHz

	micro suburban/urban
Element gain (dBi) **(Note 1)**	5.5
Horizontal/vertical 3 dB beamwidth of single element (degree)	90º for H 90º for V
Horizontal/vertical front-to-back ratio (dB)	30 for both H/V
Antenna array configuration (Row × Column)	8 × 8 elements
Horizontal/Vertical radiating element spacing	0.5 of wavelength for H 0.5 of wavelength for V
Array Ohmic loss (dB) **(Note 1)**	2
Conducted power (before Ohmic loss) per antenna element (dBm) **(Note 9)**	16 **(Note 5)**
Base station maximum coverage angle in the horizontal plane (degrees)	±60
Base station vertical coverage range (degrees) **(Notes 3, 4, 10)**	90-120
Mechanical downtilt (degrees) **(Note 4)**	10

Note 1: The element gain in row 1.2 includes the loss given in row 1.8. This means that this parameter in row 1.8 is not needed for the calculation of the BS composite antenna gain and e.i.r.p.

Note 3: The vertical coverage range is given in global coordinate system, i.e. 90° being at the horizon.

Note 4: The vertical coverage range in row 1.11 includes the mechanical downtilt given in row 1.12.

Note 5: The conducted power per element assumes 16 × 8 × 2 elements (i.e. power per H/V polarized element).

Note 6: The conducted power per element assumes 8 × 8 × 2 elements (i.e. power per H/V polarized element).

Note 8: The boresight direction is perpendicular to the ceiling.

Note 9: In sharing studies, the transmit power calculated using row 1.9 is applied to the typical bandwidth given in Table 7-1 and 8-1 respectively for the corresponding frequency bands.

Note 10: In sharing studies, the UEs that are below the coverage range can be considered to be served by the "lower" bound of the electrical beam, i.e. beam steered towards the max. coverage angle. A minimum BS-UE distance along the ground of 35 m should be used for urban/suburban and rural macro environments, 5 m for micro/outdoor small cell, and 2 m for indoor small cell/urban scenarios.

Notes accompanying the table generally clarify the usage of several parameters in the radiation pattern of the composite antenna calculus. However, it's worth mentioning two additional points:

- Note 3 indicates that the vertical coverage range of angles (90-120°) for suburban and urban cases relates to the *Global Coordinates System* (*GCS*) while Note 4 indicates that these values cover the mechanical tilt, which would mean that these values are not given in GCS but in Local Coordinate System of the BS antenna. That's why it's important to retain Note 3 and disregard Note 4 when considering these values.
- Since the proposed values of the BS antenna mechanical down-tilt is positive (10°), it is assumed that any rotation in positive down-tilt[1] is performed in clockwise direction[2].

2.7.1.1.2 Reference where to calculate the BS antenna gain

GCS is used to locate the airborne radar while LCS relates to the BS antenna panel reference. Because of the mechanical down-tilting of the BS antenna and since the antenna sector is not necessarily oriented « in front » of the aircraft[3], geometrical transformation from one coordinates system to the other one is needed to derive the direction where to calculate the gain of the BS antenna. This operation is a combination of two rotations, the first one being the mechanical tilt and the second being the azimuth. If different BS of the same environment (urban or suburban) operate with the same mechanical down-tilt, their different azimuthal positioning with respect to the airborne radar will lead to different transformations to get in LCS.

2.7.1.2 Operational characteristics

2.7.1.2.1 BS deployment characteristics

Tables 1 and 2 below provide the deployment-related parameters of IMT systems for the frequency band 6 425-7 125 MHz. Urban and suburban micro scenarios are considered in this study.

TABLE 2

Deployment-related parameters for bands between 10 and 11 GHz

	Urban/suburban micro
Deployment density (Note 1)	D_{BS_U} =30 BSs/km^2 urban / D_{BSSub} =10 BSs/km^2 suburban **(Note 2, 3)**
Antenna height	6 m urban / suburban
Sectorization	1 sector
Indoor base station deployment	n.a.
Indoor base station penetration loss	n.a.
Typical channel bandwidth	100 MHz

[1] To go from LCS to GCS.

[2] In particular when deriving any gain of the BS antenna (in LCS).

[3] i.e. same azimuth of the airborne radar if another reference is taken (e.g. North) or 0° if the radar is the reference of the azimuth axis.

	Urban/suburban micro
Network loading factor (base station load probability X%) (see section 3.4 below and Rec. ITU-R M.2101 Annex 1, section 3.4.1 and 6)	20% A network loading value of 20% would normally represent a typical/average value for the loading of base stations across a network (or part thereof), and should be used for sharing and compatibility studies that are considering a relatively wide area (e.g. a large city, province, country or satellite footprint).
TDD / FDD	TDD
BS TDD activity factor	75%

2.7.1.2.2 BS deployment in small area

For IMT deployments over areas such as visibility of a radar system (i.e. area locations whose elevation angle towards the aircraft is positive) corresponding to hundreds/thousands km^2, it is recognized that IMT base stations will not be deployed at the same high density across the whole area, that's why the deployment density values in the Table 2 needs to be adjusted. Two additional parameters were proposed by WP5D: R_a (%) the ratio of coverage areas to areas of cities/built areas/districts and R_b (%) the ratio of built areas to total area of region in study. Doc 5D/716 Annex 4.4 of the Chairman's report provides two R_a/R_b values options depending on the size of the simulation area (see below Table).

TABLE 3

BS deployment in large area for 10-11 GHz band

	Options[4]	**Hotspots (outdoor)**
Ra	1	7% Urban 3% Suburban
Rb (depending on the area under study)	1	5% (area < 200 000 km^2) 2% (200 000 - 1 000 000 km^2) 1% (area > 1 000 000 km^2)
	2	2.5% (area < 200 000 km^2) ** 2% (200 000 - 1 000 000 km^2) 1% (area > 1 000 000 km^2)

According to the above table, $R_{a\ urban}$ =7% and $R_{a\ suburban}$ =3%. Since the analysis in this document deals with a very small area (few thousands km^2) and in accordance with the work undertaken during the previous cycle (TG 5/1) whose an extract is provided as follows:

[4] The Ra and Rb values used in the sharing and compatibility studies should be provided together with the results of studies, for the purpose of comparison, as well as information on which specific geographical location the analysis is applicable to.

For each satellite, the corresponding footprint (with area S) is centred on the urban area, and the number of BS within the footprint is calculated using one of the two following examples, depending on the specific city area considered (with the assumption that Rb=1 within 1 000 km²):

Example A (no separation between urban vs. suburban)	**Example B** (separation of urban vs. suburban)
If S < 1 000 km²: **Nb of BS1 = S*(Ds_urb * Ra_urb + Ds_sub * Ra_sub)**	If S < 200 km² (urban only, with Rb =1): **Nb of BS1 = S*(Ds_urb * Ra_urb)**
	If 200 km² < S < 1 000 km² (urban & suburban, with Rb = 1): **Nb of BS2 = Nb of BS1(with S=200) + (S-200)*(Ds_sub * Ra_sub)**
If S > 1 000 km²: **Nb of BS2 = Nb of BS1(with S=1 000) + (S-1 000)*(Ds_urb * Ra_urb + Ds_sub * Ra_sub)*Rb**	If S > 1 000 km²: **Nb of BS3 = Nb of BS2(with S=1 000) + (S-1 000)*(Ds_urb * Ra_urb + Ds_sub * Ra_sub)*Rb**

This would mean that the number of micro BSs would be derived over a full urban area within 200 km^2 with $R_{a\ urban}$ =7% and R_b =100% (as representative of a city) and suburban area with $R_{a\ suburban}$ =3% and R_b =100%. Such approach was followed for the static study in Doc 5D/1316.

For the dynamic analysis, the situation is different as the number of hotspots depends on the simulation area *S*:

- Case #1: If *S* is chosen to be the visibility area of the aircraft, this latter varies with the position of the airborne radar (denoted *M*) *S(M)* along the path. Applying R_a/R_b factor to derive the number of BSs *N* within a given location would artificially make *N* vary upon the visibility area *S(M)* (if several visibility areas *S(M)* contain the same location for an IMT deployment)
- Case #2: If *S* is extended to a larger zone than the visibility area e.g. the concatenation of every visibility areas of the aircraft along its path under study, a rule on how to deploy IMT BSs in a realistic manner as a function of the visibility of BSs towards the aircraft should be elaborated. The term "realistic" refers to a deployment of these micro BSs in high population density (urban, suburban) locations. This rule should also comply with R_b value e.g. if R_b=100% the built-up area ration should be close to 100%.

In light of inconsistency R_a/R_b method would generate for case #1 or the impossibility to meet multiple constraints for case #2, R_a/R_b cannot be directly applied for a dynamic study where the simulation area varies. Population density thresholds should be carried out in conjunction of R_a/R_b factors.

If population density thresholds T_{sub}, T_{urb}, $Ts_{sub,Rb}$ to distinguish urban from suburban or full built-up from R_b areas were selected to match the number of BSs derived from R_a/R_b factors, T_{sub}, T_{urb} would be too small to comply R_b=100% constraints. On the contrary, if T_{sub}, T_{urb} comply with R_b=100%, the resulting number of micro BSs would be much smaller than the one achieved R_a/R_b with factors even though $Ts_{sub,Rb}$ is the lowest value (1 inhabitant/km^2). What appears to be a tricky issue is not when recalling that R_a/R_b values resulted from compromise in ITU-R and recalling that "*when the size of area under the study is very large assuming very large satellite-footprint or countries the Rb value needs to be decreased to reflect sparse population density of the countries*". This quote suggests that depending on the population density distribution, countries R_b could be higher or lower than the value recommended by WP5D. This seems to be the case for Brazil and achieving lower number of micro BSs than what would have been obtained with R_a/R_b factors by complying with R_b=100% would not be irrelevant. In a such case, fixed population density thresholds methodology is applied for the sharing study and the figures are computed so that it tends towards R_b=100%. An illustration of a

100% built-up area through surface element unit filtering[5] T_{sub} is provided in the below pictures of the cities (and their vicinity) within the simulation area.

FIGURE 1

Rio Janeiro (T_{sub} =7000 inh/km^2)

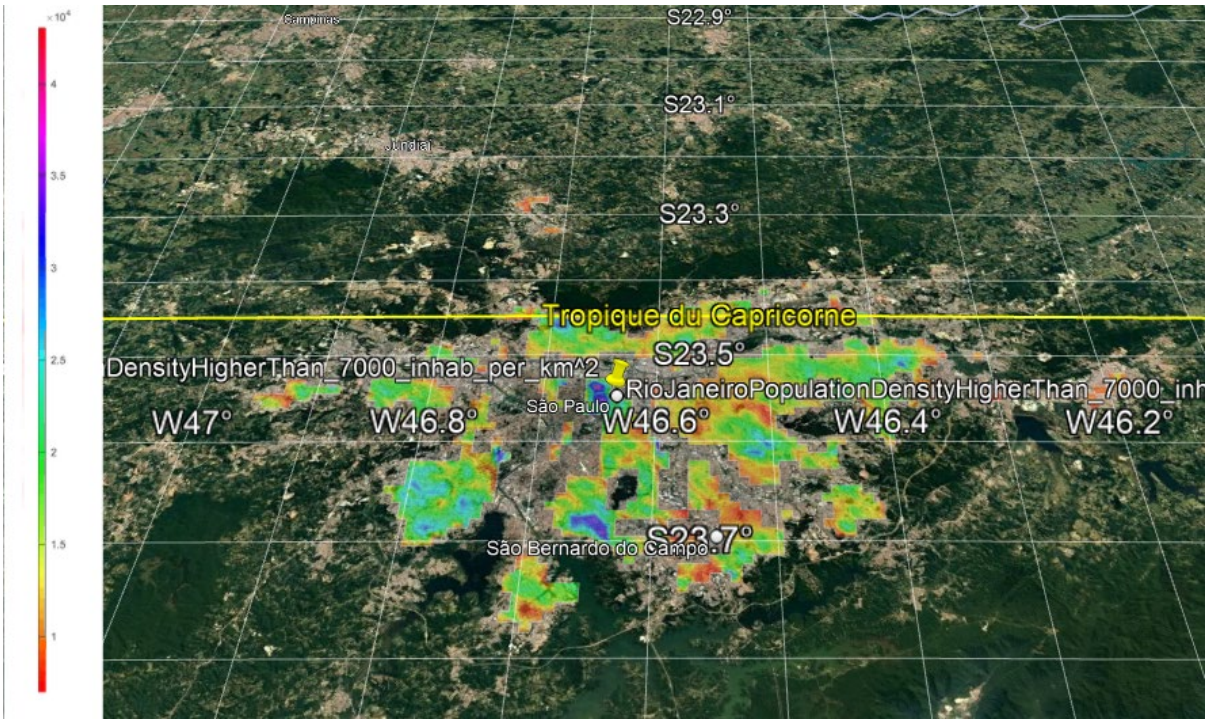

FIGURE 1

Sao Paulo & suburbs (T_{sub} =7000 inh/km^2)

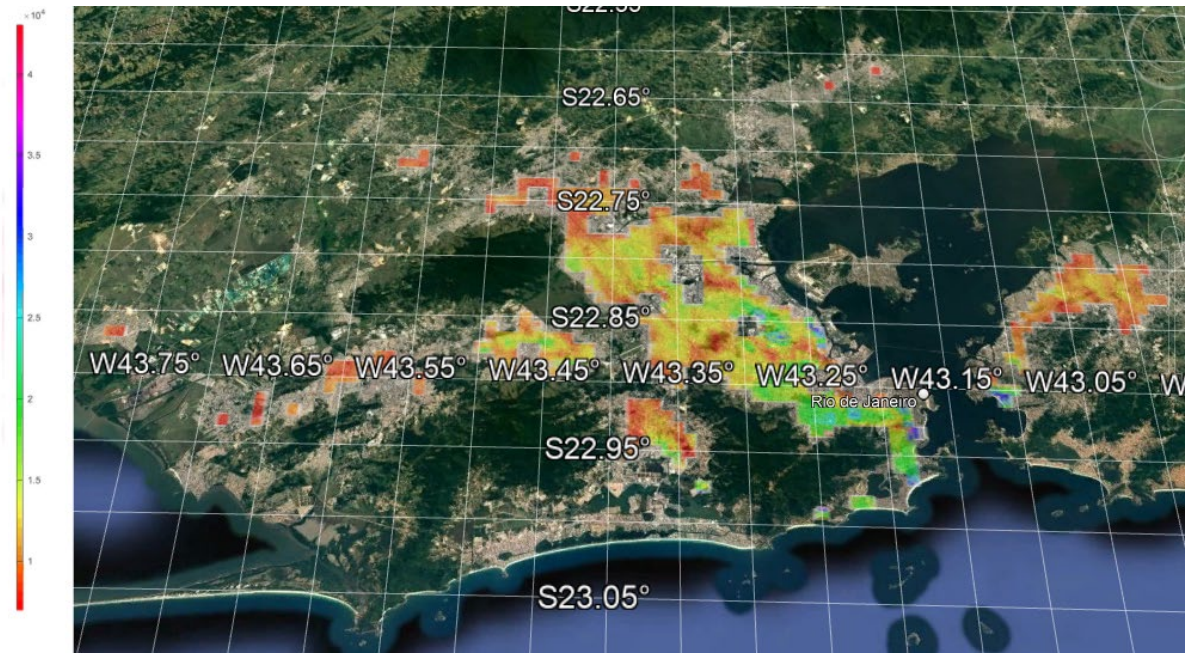

[5] By retaining only tiles that have equal or higher population density than T_{sub}

The third population threshold $Ts_{sub,Rb}$ (suburban in sparse populated areas) could be set to 100 inhabitants/km^2 in accordance with the assumption taken for a research paper[6].

When applying such methodology, the resulting total number of hotspots within the entire country would be lower than the value obtained when sticking strictly to R_a/R_b factor for the computation of the amount of micro BSs.

2.7.1.2.3 Calculation of BS radiated power

Work undertaken during the previous cycle (Document 5-1/124) and also in 3GPP indicates the need to ensure that the total array directivity is equal to 0 dB minus any loss related to the antenna array (efficiency, ohmic, coupling, mismatch and/or insertion loss…). The calculation of the *Total Integrated Gain (TIG)* over the whole sphere for the single radiating element leads to around -2 dB, indicating that the 2 dB array ohmic loss provided in above table is already included in the analytical expression of the single element radiation pattern. Performing the same kind of calculation for the composite antenna where the beam-steering is generated within the vertical and horizontal coverage leads to an overall range of variation -2..0 dB for *TIG* and is depicted in the below picture for the suburban and urban micro environments.

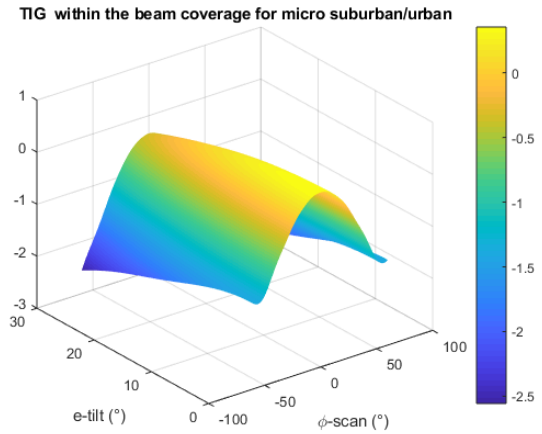

This small variation of the TIG in negative values is consistent with array (mismatch, coupling, ohmic) losses affecting the composite antenna in the beamforming process. Therefore normalization of the composite antenna gain for the IMT micro BS is not needed as the current analytical expression (from Recommendation ITU-R M.2101-0 and whose beamforming characteristics are extracted from Table 1) captures the losses related to antenna.

Based on the parameters set by WP 5D and using formula given in Rec ITU-R M.2101-0, the distribution of BS antenna gain for different elevation angles but towards the airborne radar ($i.e. \varphi = 0°$ in GCS) is generated over 50 000 runs (i.e 50 000 random directions of the beam are built over the cone of coverage – delimited by horizontal -60..60° and vertical bounds 90..100/120° in GCS -) displayed for suburban and urban environments in terms of *complementary cumulative density function (ccdf)*: It should be noted that the location of azimuth BSs with respect to the aircraft ones is (uniformly) randomly generated within -180..180° range. This means that the BS antenna gain is calculated over the whole BS azimuth range, i.e. -180 to 180 degrees.

[6] https://sedac.ciesin.columbia.edu/urban_rs/PozziSmall2002.pdf

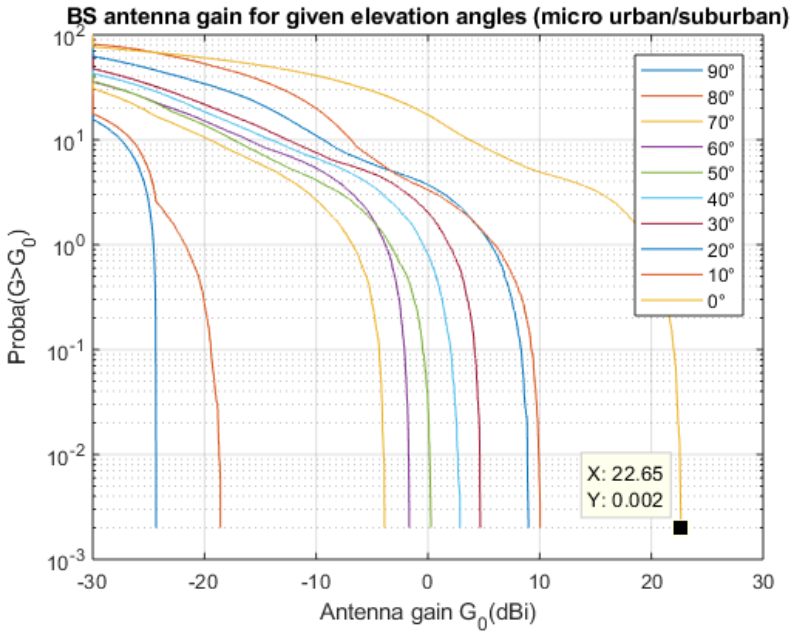

One could find out:

- That for higher elevation angles (0° related to the horizon, 90° related to the zenith), the quantile for which there is a percentage exceedance is decreasing. Such fact comes from the down-tilt effect of the micro BS which results in lower gain above the horizon.
- The lowest value of the curve (related to 2.10^{-2} percent) matches with the number of samples[7] (50 000).

Finally, the radiated power of micro BS (in urban and suburban areas) can be calculated by adding the conducted power (from parameters of Table 1) using to the BS antenna gain derived earlier. It should be noted that due to multiple UEs (3 per sector) served by the same micro BS sector, the conducted power of micro BS is equally apportioned (as channel bandwidth is equally shared by the three terminals) when radiating the power to three different terminals.

2.7.1.2.4 Calculation of UE radiated power

Since UE operates with non-AAS. the power control algorithm is independent of the orientation of the UE antenna. Following Recommendation ITU-R M.2101-0, power control algorithm is applied to derive the transmit power P_t as follows:

$$P_t = min\left(P_{CMAX}, 10log_{10}(M_{PUSCH}) + P_{0\_PUSCH} + \alpha.PL\right)$$

It has to be noted that *PL* between UE and BS as defined in this Recommendation also covers other losses than pathloss, i.e. body loss and (BS and UE) ohmic losses, if any but also the UE and BS antenna gains[8] (respectively towards BS and UE). *PL* parameter can then be understood as a coupling loss component. The input parameters required to derive the UE output power are extracted from Document 5-1/36 .:

[7] 2.10^{-2}=1/50000.

[8] Calculated with the normalization factor.

TABLE 4

UE Power control algorithm input parameters

Number of UEs per sector	N/A	3
Channel bandwidth	MHz	100
Maximum user terminal output power P_{CMax}	dBm	23
Transmit power target value per RB, P_{0PUSCH}	dBm/180 kHz	-92.2
Pathloss compensation factor α	N/A	0.8
UE Antenna gain	dBi	-4
UE Body Loss	dB	4
Indoor user terminal penetration loss	dB	Rec. ITU-R P.2109

The table shows that

- in any case involving indoor user, the penetration loss needs to be calculated when deriving radiated power towards the aircraft, using Recommendation ITU-R P.2109 with random location variability percentage ranging 1..99%. The building entry loss between serving BS and UEs should be calculated using models from Report ITU-R M.2412-0,
- every UE is allocated 1/ (Number of UEs per sector) of the channel bandwidth, i.e. around 33 MHz.

2.7.2 Technical and operational characteristics of Radiolocation operating in the frequency band 10 000-10 500 MHz[9]

Recommendation ITU-R M.1796-3 provides the characteristics of and protection criteria for airborne radars operating in the radiodetermination service in the frequency band 8.5-10.5 GHz.

Although key airborne radar modelling parameters for sharing studies are summarized in Table 5, below.

TABLE 5

Airborne Radar Modelling Parameters for Sharing Studies

Characteristics	Units	System A12
Tuning range	MHz	8 500-10 500
Protection criterion I/N	dB	-6
Antenna main beam gain	dBi	35-42
Antenna horizontal scan type (continuous, random, sector, etc.)		±120°
Antenna vertical scan type (continuous, random, sector, etc.)		±120°

[9] Although the systems operate in 8 500-10 500 MHz, the sharing study with IMT relates to the frequency band from AI 1.2 for a possible IMT identification i.e. 10 000-10 500 MHz.

Characteristics	Units	System A12
Antenna side-lobe (SL) levels (1st SLs and remote SLs)	dBi	14-19 dB below peak gain
Antenna height		9 km
Receiver noise figure	dB	6

Any sharing study dealing with an active electronically scanned array should require modelling beamforming approach by implementing a radiation pattern for every beam-steering. Although ITU-R Rec M.1796-3 refers to ITU-R Rec M.1851-1 for system A12 on mathematical model for radar antenna pattern, there is no detailed[10] guidance for designing planar array complying with the expected requirements over the antenna gain e.g. no grating lobes occurrence within ±90° off-axis angle (azimuth and elevation), low peak gain reduction of the composite antenna with high beam depointing. Moreover, noting that ITU-R Rec M.1851-1 states that *a mathematical model is required for generalized patterns of antennas for interference analyses* ***when no specific pattern is available for the radiodetermination radar systems***, and *that, in the absence of information concerning the antenna patterns of the radiodetermination radar system antenna involved, one of the mathematical reference antenna models described in Annex 1 should be used for interference analysis,* the study aims at providing a mathematical model based on real mounted antenna for aircrafts used by several administrations. The physical property of the antenna is ensured. The considered geometry of antenna phase array is a rectangular alignment of single elements for this study. The detailed parameters used to design such pattern is given as follows:

TABLE 6

Characteristics of the radar antenna array

Parameters	Units	Value
Single element 3dB beamwidth	°	100 for both azimuth & elevation
Back lobes level	dBi	-30
Single element peak gain	dBi	6
Number of horizontal elements	N/A	36
Number of vertical elements	N/A	36
Horizontal beam scan range	°	-60..60
Vertical beam scan range	°	-60 ..60
$\left(\frac{d}{\lambda}\right)_{H,V}$	N/A	(0.53, 0.52)

The characteristics of the single element composing the electronic scanned array is also provided below in order to ensure that the low sidelobe levels above ±90° off-axis remove any grating lobes emergence within the pattern despite the element spacing ensures the no grating lobes conditions[11]:

[10] Although it states in page 22 *even if the array lattice is λ/2 among the elementary radiating elements in the array, sidelobes of the grating lobes of the mainlobe, situated at −90° and +90° from the mechanical antenna boresight, disturb the array pattern*

[11] $\frac{d_z}{\lambda} < min\left(\frac{1}{1-cos\theta_{e-tilt}}, \frac{1}{1+cos\theta_{e-tilt}}\right)$ and $\frac{d_y}{\lambda} < min\left(\frac{1}{1-sin\varphi_{scan\ radar}sin\theta_{e-tilt}}, \frac{1}{1+sin\theta_{e-tilt}sin\varphi_{scan\ radar}}\right)$

TABLE 7

Single patch element physical features

Parameters	Length	Width	Height	Frequency	Relative dielectric constant ε_r
Value	0.906 cm	1.186 cm	0.1588 cm	10 GHz	2.2

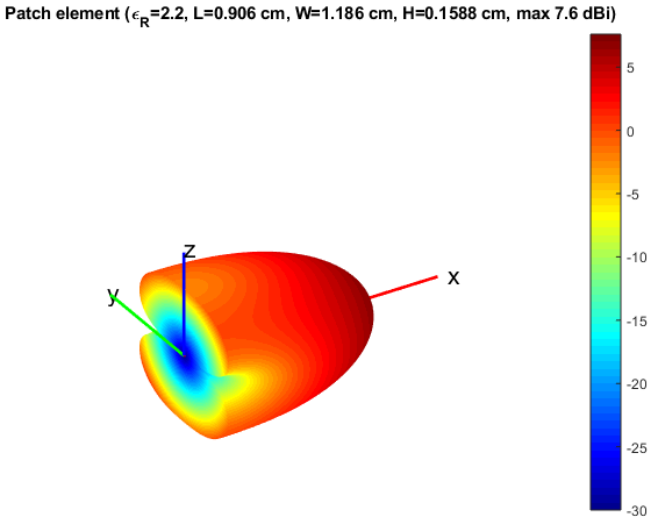

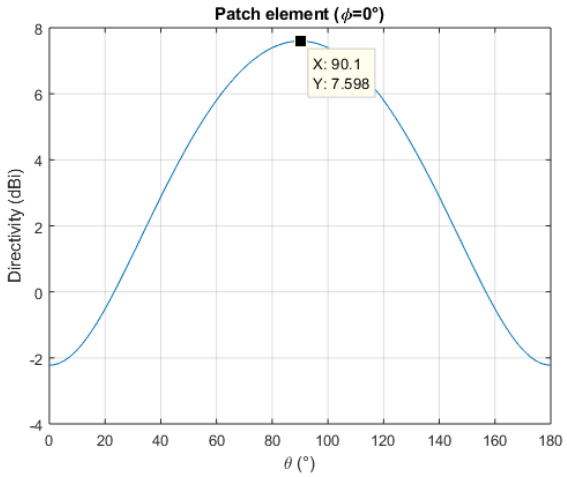

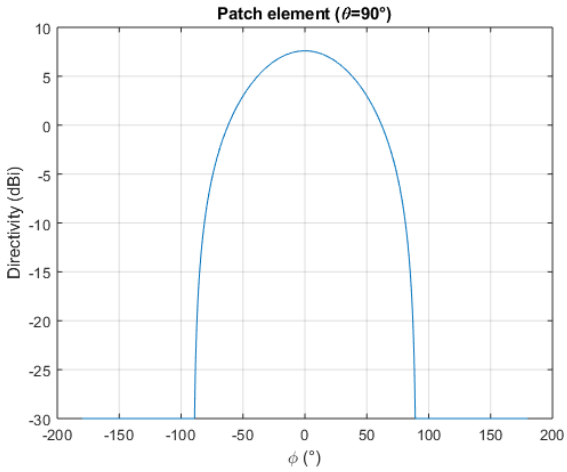

The fact that the fall down of the radiation level occurs more in the horizontal plane than in the vertical plane of the single element radiation pattern explains why the vertical element spacing of the planar array is a little smaller (0.52) than the mathematical conditions for removing grating lobes emergence with the extreme beam depointing ($\pm 60°$) due to the array factor of the composite antenna.

A windowing signal process is also applied to the receiver part of the antenna radiation pattern because the aircraft needs to maximize the collection of the information about the direction finding within a larger main lobe. The mathematical expression of the time response is given by: $h[n] = e^{-\frac{1}{2}(n\sigma)^2}$ where $\sigma = 0.04$.

From the above information (array factor, patch element, weighting function), a plot of the gain of the composite antenna is depicted without any depointing

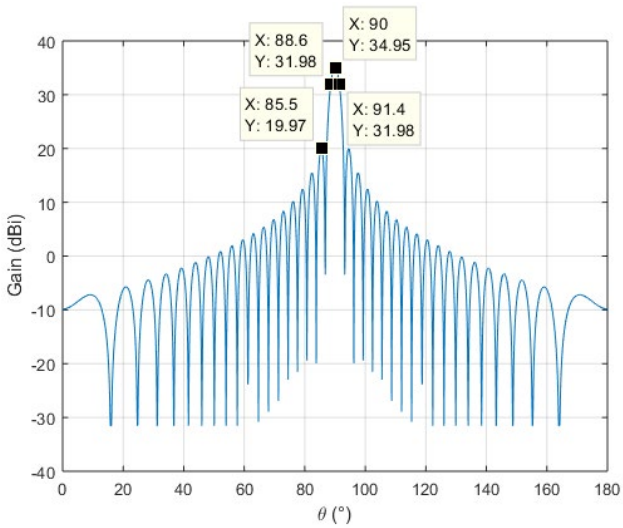

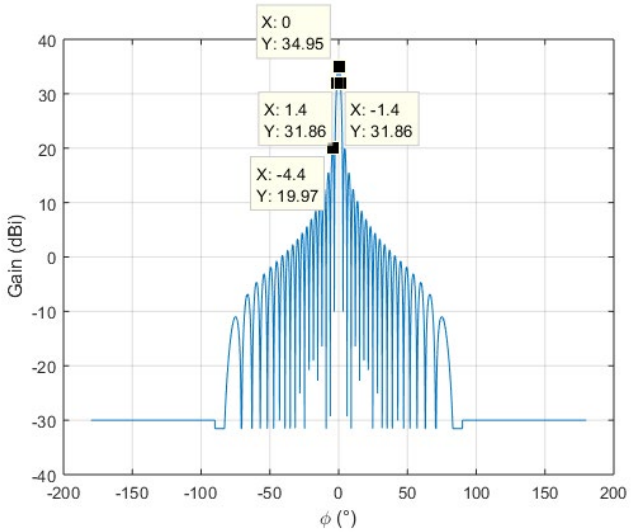

The peak gain of this antenna belongs to the range of values 35-42 dBi given in Table 1 from ITU-R Rec M.1793-3 for System A12. Moreover, the first sidelobe levels achieved for this pattern (34.95-19.97≈15dB) also falls within the range of values recommended in the same Table (14-19 dB). Finally, 3D the representation of the antenna pattern with/without beam pointing is provided for the aircraft and shows the absence of grating lobes (in particular for the extreme beam-steering to the range of scanning angles).

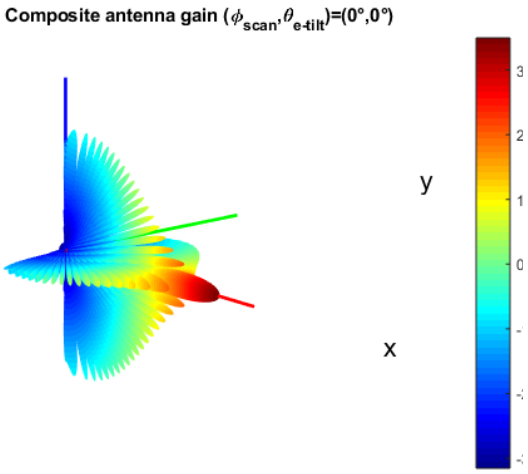

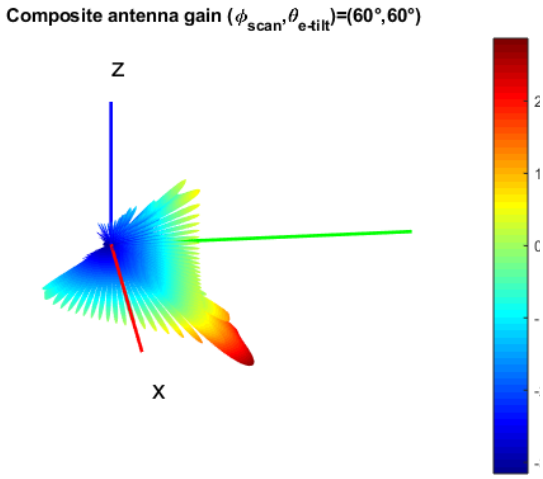

2.7.3 Propagation assumptions

2.7.3.1 Background

In accordance with Document 5D/722 - Reply liaison statement to Working Party 5D - WRC-23 agenda items 1.1 and 1.2 propagation model recommendations, from WPs 3K and 3M, Recommendation ITU-R P.528 should be considered for the evaluation of interference between airborne stations and those on the surface of the Earth, whose revision at the Study Group 3 meeting in July 2021 was proposed (see Document 3/51(Rev.1)). Since no guidance was provided on the appropriate percentage of time to be used as an input of Recommendation ITU-R P.528-5, it is

proposed to study the sharing for a range of percentages of time and compare them with the Free-Space-Loss propagation model (Rec. ITU-R P.525). According to the discussions held for the protection of Radio-navigation from IMT HIBS in 2.7 GHz (See Chairman Report Document 5D/1078 Chapter 4 Annex 4.30), *"Propagation model used is Recommendation ITU-R P.528 with a time availability value of 0.05 (5%)."*

It is then proposed to consider 5% as well as 10% for the percentage of time for the sharing study as preliminary analysis.

2.7.3.2 Clutter loss

Based on the latest LS from WP 3K-3M (5D/722), *the development effort to lower the applicable frequency range to below 10 GHz, will continue unabated during the upcoming intersessional period (See Annex 6 to Working Party 3K Chairman's Report, Document 3K/178) in Correspondence Group 3K-3M-12. In the interim WPs 3J, 3K and 3M note that the existing slant path model in section 3.3 of Recommendation ITU-R P.2108, for which the frequency range of applicability is from 10 to 100 GHz, may be extrapolated downward in frequency for WRC-23 agenda items 1.1 and 1.2 co-existence studies*.

There was a high debate during previous WP 5D on whether a proponent should use the current Earth-space clutter loss model Recommendation ITU-R P.2108-1 below 10 GHz or consider any material in Document 3K/178. In absence of agreement on this issue and noting the content of the liaison statement (LS), France is of the view that it is important, for a sake of transparency and to be consistent with Document 5D/722, to provide the results of the sharing studies by using the existing slant path model in section 3.3 of Recommendation ITU-R P.2108 with an extrapolation downward in frequency for these studies. France also recognizes the importance of keeping in the studies the other clutter loss model under consideration in CG 3K-3M-12 in light of the content from Document 3K/178. For that reason, two models are tackled in the assessment of the interference:

- Recommendation ITU-R P.2108-1 (Section 3.3) extended to the bands below 10 GHz applied to all small cell BSs because their antenna height (6m) is below the clutter
- the model in Document 3K/178, is an update of the loss model of ITU-R P.2108-0 for *including a ground station height dependence up to 20 m (though maximum 5 m below the clutter height*), and *extending* the applicability frequency range to 0.7-100 GHz. The computation of such model requires further comments on its input parameters:

  i. **Location variability parameter** (%) captures the diversity of positioning of the ground station with respect to the obstructing building (regarding the link ground station – aircraft): *LoS/NLoS*. That's why the formula of the new proposed model **can be used within the whole range of percentage (1..99%)** without distinguishing Base Station below/above the clutter because they are always higher buildings in the vicinity of a building hosting a BS at its top and also because the below/above rooftop ratio gave a coarse hint/a rule of thumb of how to compute clutter loss for P.2108 current model not accounting the shielding clutter height & ground station antenna height as parameters.

  ii. **Ground station height** h_{BS} is given as fixed parameter and relates to various configurations such as a location at the roof for a lower building than h or in facade of the building when it's higher than h.

iii. **<u>Shielding building height</u>**: Although BS antenna height is given for every environment (6m respectively for urban and suburban areas), the building shielding height parameter is not provided. However, Recommendations ITU-R P.452-17 and ITU-R P.2108-1 provide information on nominal/typical heights for clutter in various environments through Table 4 whose part is extracted below:

TABLE 8

Clutter characteristics (from Recs. ITU-R P.452-17 & ITU-R P.2108-1)

Environment	Nominal height (m)
Suburban	9
Dense suburban	12
Urban	20
Dense urban	25

Environment	Nominal height (m)
Suburban	10
Dense suburban	N/A
Urban	15
Dense urban	20

As can be seen from the above tables, differences in values are noticeable (typical urban cases range from for 15 m in Recommendation ITU-R P.2108-1 to 20 m for Recommendation ITU-R P.452) for the considered environment recommendation. Moreover, if a first glance at the naming of the environment under study for the IMT deployment let us think that the sharing is only dealing with urban and suburban and not considering at all dense urban and dense suburban, it should be understood that this naming is general and could also cover the "dense" sub-category of each of them (urban, suburban). Unfortunately, when dealing with these multiple cases, there are three emerging problems:

- There is a missing information on one of these sub-categories (dense suburban) for Recommendation ITU-R P.2108
- Which apportionment between the regular and the dense parts of the same environment (suburban/dense suburban and urban/dense suburban) should be decided when defining these clutter heights?
- A minimum 5 m between the shielding building height and the ground station height is required for the model described in the preamble of the section 3.3 of the Annex 1 of Document *3K/178 6 Annex 6*,

For the first bullet, since the BS (ground) station antenna height (20 m) is always much higher than the building shielding height (9, 10 m respectively for Recs. ITU-R P.452-17, ITU-R P.2108-1 suburban and 12 m for dense suburban), it is proposed to use **<u>10 m for suburban</u>**.

For the second bullet, due to lack of information on how to proceed, a way forward would be to take a middle ground between every sub-category and also between the two differences reference tables (from Recs. ITU-R P.452-17 and ITU-R P.2108-1). The middle ground for the urban case between those two recommendations would be 17.5 m (between 15 m and 20 m) and for the dense urban case would be 22.5 m (between 20 m and 25 m). Hence the overall middle ground between dense urban and urban would be **<u>20 m</u>** (between 17.5 m and 22.5 m) **<u>for urban</u>**.

For the third bullet, although there is only 4 m between clutter height for the suburban (10 m middle ground) case and the BS antenna height (6 m) and not a 5 m minimum value, trying to use the proposed model under consideration from Annex 1 of Doc. *3K/178 6 Annex 6* would lead to the following result for three exemplary (elevation angle) cases:

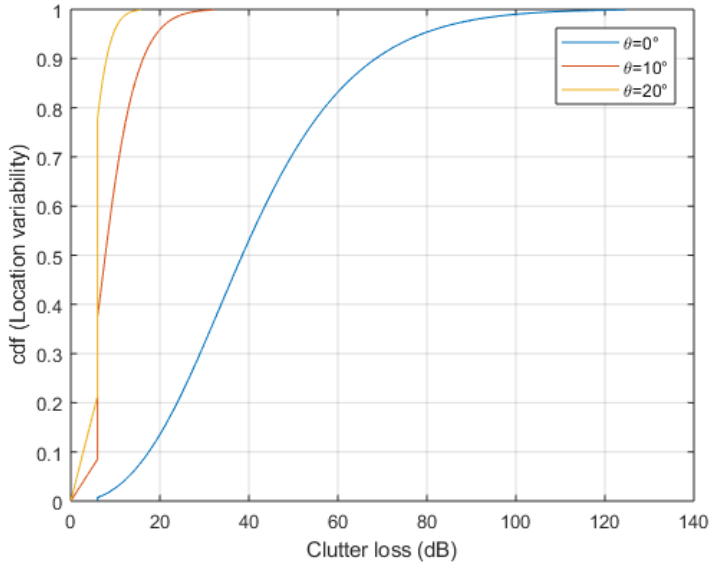

and appears not to cause any issue on the curves obtained from the time the shielding building height is higher than the height of the ground station. This leads to assume:

- for the urban area, a shielding building h_s=*20 m* (as a middle ground between dense urban and urban as well as the different references i.e. Recs. ITU-R P.452-17 and ITU-R P.2108-1)
- for the suburban area, a shielding building h_s=*10 m* (as a middle ground between dense suburban and suburban as well as the different references i.e. Recs. ITU-R P.452-17 and ITU-R P.2108-1)

2.7.3.4 Other losses

Concerning the loss due to polarization discrimination, during the previous cycle of studies, TG 5-1 investigated that topic[12] and drew the following conclusion:

For aggregate interference studies, based on the polarization discrimination equation (see Recommendation ITU-R F.1245), a 3 dB average polarization loss could be applied under the following assumptions:

- *The aggregate interference is resulting from off-axis emissions of a large number of BS/UE, with a uniform distribution of tilt angle between 0 to 180 degrees and equal probability for both senses of rotation;*
- *There is no domination of interfering power level for one or a limited number of the BS/UE with the same sense of rotation or the same tilt angle of polarization ellipse.*

Accounting the large size of the simulation area, the active IMT systems will be numerous and geographically distributed in a way that whatever if IMT systems radiate wave with the same linear polarization or circular polarization with different orientations (left/right hand) with equal distribution, polarization loss will be 3 dB to meet the above first condition.

[12] Under agenda item 1.13 from WRC-19.

2.7.4 Technical Analysis

2.7.4.1 General Methodology

2.7.4.1.1 Mobility of the aircraft

As described in Recommendation ITU-R M.1796-3, airborne radars operate over a range of scanned elevation angles below and above the horizon to provide *long-range surveillance, target tracking and Synthetic Aperture Radar imagery*. The aircraft is assumed to fly over the international waters for patrol operation where the radar antenna is scanning in different angular directions, following the range of electrical tilt and phi-scan angles. Without precluding the capability of the system to tune/change its altitude and speed during the mission, the analysis considers that the aircraft operates at a fixed height above the sea mean level (9000 m) with a constant velocity (250 $m.s^{-1}$). The path has been defined through path segments (whose geodetic coordinates are provided in the below table) for which loxodrome is applied to get consistent distance & trajectory of the aircraft.

TABLE 9

Geodetic coordinates of the end of the path segments

Path segment	**1**	**2**	**3**	**4**	**5**	**6**	**7**	**8**	**9**
start of path segment	-23.55°N -43.75°E	-23.6°N -44.00°E	-23.7°N -44°E	-23.75°N -44.6°E	-23.8°N -44.7°E	-24.1°N -44.8°E	-24.3°N -45°E	-24.4°N -45.5°E	-24.5°N -45.75°E
end of the path segment	-23.6°N -44.00°E	-23.7°N -44°E	-23.75°N -44.6°E	-23.8°N -44.7°E	-24.1°N -44.8°E	-24.3°N -45°E	-24.4°N -45.5°E	-24.5°N -45.75°E	-24.6°N -46°E

The non-homogeneous nature of the national waters delimited by coast and small islands was also accounted to ensure that any geographical position of the aircraft within its trajectory belongs to the international area. The trajectory under study starts at (23.55°S,43.75°W) and stops (24.6°S, 46°W) for around 273 km length, as depicted in the below figure (green curve). Thus, at a constant speed, a little more than 18 minutes is required for the aircraft to reach the end of the path.

One could notice that for every position of the aircraft, since IMT BSs can be located everywhere in populated environments in coastal areas, there is no monotonic behaviour of the distance between the aircraft and the sources of interference.

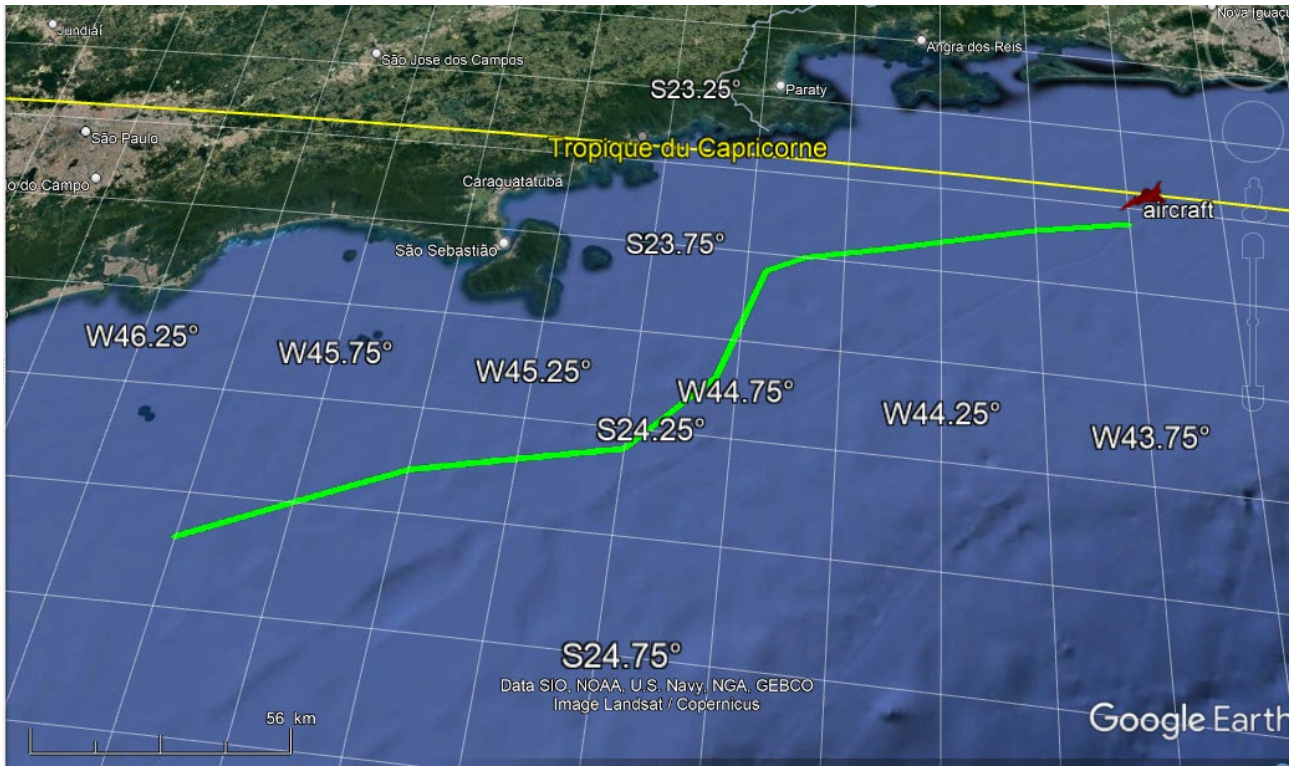

2.7.4.1.2 Operation of the radar antenna

As indicated in the introductory part, France has some territories in Region 2, e.g., French Guiana and aircrafts are assigned to cover a variety of missions such as detecting prohibited fishing, gold mining incident or identify any illegal immigration and unlawful flying over the French overseas territory. In cooperation with other radiolocation systems (ground radars), they can insure the air surveillance coverage. Aircraft may also patrol in areas outside national borders. One typical scenario for the French airborne radar would be an aircraft surrounding the coastlines of South American but still located outside territorial waters and whose antenna is not directed in any territory of another country. In order to fulfil those missions, active electronically scanned array installed inside its cone nose is used to detect and track areas of interest. As highlighted in Section 2.3 from Rec M.1796-3, such active antenna *do have the capability to perform different radar tasks (e.g. tracking and scanning and tracking of multiple targets)* ***simultaneously***. The spatial scanning volume of the array is featured over azimuth (denoted φ_{scan}) and elevation (denoted θ_{e-tilt}) range of values given in ITU-R Rec M.1796-3 (e.g. -60..60° for System A12). The typical procedure of steering angles is also described in the same Recommendation with a *scanning line by line or circles of a pencil beam is replaced by signal processing with adaptive tracking and scanning*. In other words, the airborne radar performs beam-forming when scanning every angle solid using digital narrow beams. The detection (of any object within this angular direction) process of the radar is generally improved when performing a spatial overlap of successive pencil beams (main lobe) in order to increase the correlation of the data collected by the aircraft. A small overlapping between adjacent beams (main lobe) is sufficient to achieve such goal e.g. by sampling spatial spacing of the electronic beam for φ_{scan}et θ_{e-tilt} strictly lower than the 3dB beamwidth in any direction (azimuth and elevation). The detection *and tracking of multiple targets* is performed through multiple beams. Indeed, the radar transmits a number of pulses toward multiple targets to increase the probability of detection. Depending on the processing power allocated per pencil beam,

the antenna is able to receive simultaneously in different directions θ_1 to θ_N . Up to 30-60[13] targets can be tracked in the detection area. The smaller the number of targets to track, the higher the maximum range as well as the probability of detection.

As mentioned above, multiple modes are considered to fill a mission. One of them so called ***Look Down Mode*** (*LDM*) is important as it addresses the large reflection issue encountered when the radar antenna points to the ground: the clearance of the clutter using *Fast Fourier Transform (FFT)* and windowing techniques[14] enables the detection of ground targets of interest (the electrical tilt of the beam is always oriented at or below the horizontal $e_{tilt} \geq 0°$ below the horizontalof the aircraft). For this study, the aircraft operates under *LDM* and $-60 \leq \varphi_{scan} \leq 60°$, and $e_{tilt} \geq 0°$.

While scanning vertically and horizontally the radio horizon during the flight, the antenna beam of the aircraft can cover not only water areas outside a country but also a part of the in-land area, crossing populated areas such as cities like Sao Paulo, Rio Janeiro. In light of the curvature nature of the path, the orientation of the aircraft (defined by its directional speed) varies and needs to be considered in the computation of the radiation pattern[15]. A 25dB contour antenna footprint is plot for the sake of readability (the visibility antenna footprint is assumed in the analysis for the computation of the aggregate interference) as examples for two different positions of the aircraft, resulting in achieving two different pointing angles, showing that in-land or water areas can be scanned by the antenna (main lobe) depending on the orientation of the beam from the active electronic scanned array. The numerous transparent spacings (denoting lower gain than the 25 dB contour plot) between lobes of the antenna footprint reflect numerous nulls obtained in the array factor with a high number of single elements (36 for both horizontal and vertical lines).

[13] https://www.radartutorial.eu/20.airborne/ab04.en.html

[14] referred in ITU-R Recommendation M.1796-3 as *a fast Fourier transform-beamforming or space time signal processing.*

[15] The scanning angles being defined in the local reference of the aircraft antenna, whose orientation is a function of the path.

FIGURE 3

Aircraft antenna at (-23.55°N, -43.75°E) pointing its beam at (φ_{scan}, θ_{e-tilt})=(60°,4°)

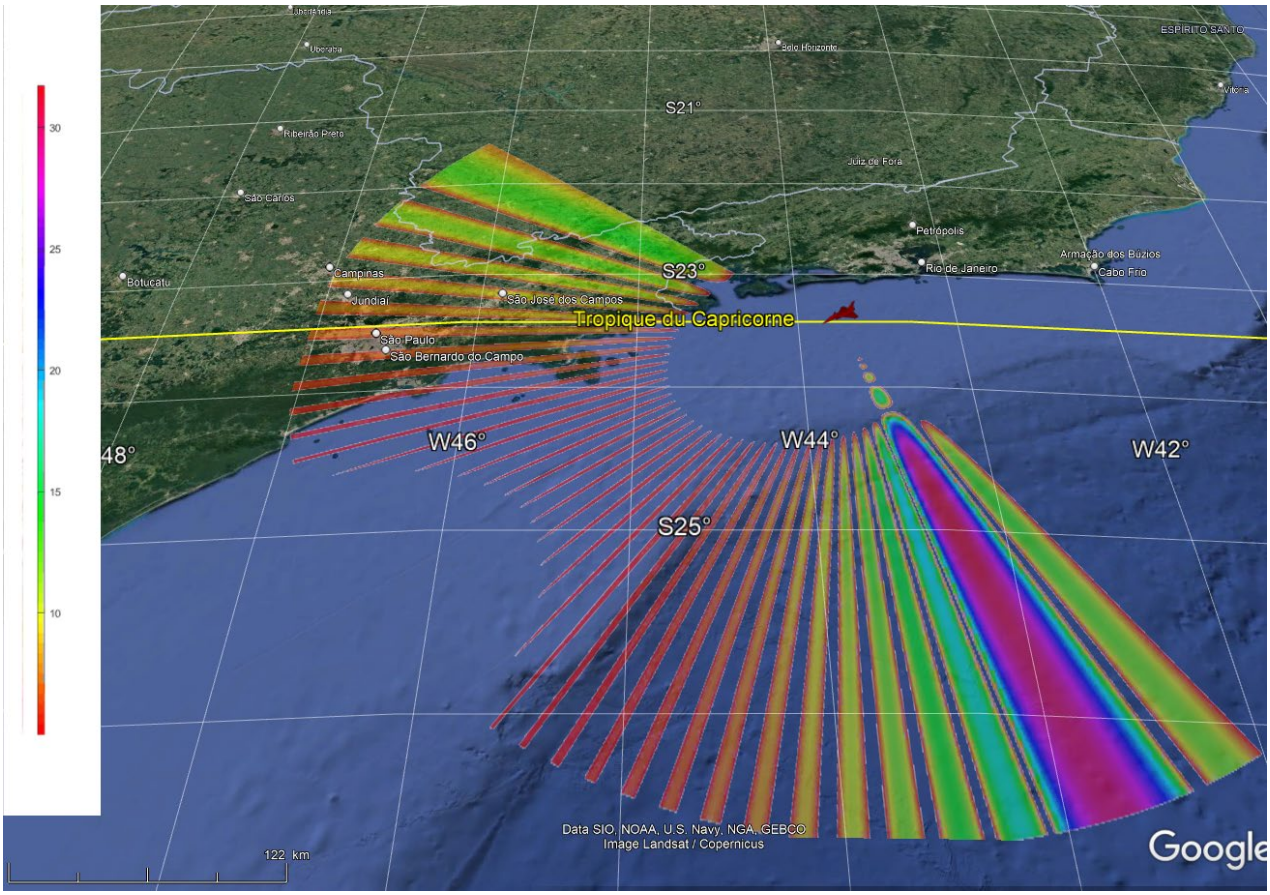

FIGURE 4

Aircraft antenna at (-23.5788°N, -43.8942°E) pointing its beam at (φ_{scan}, θ_{e-tilt})=(-60°,4°)

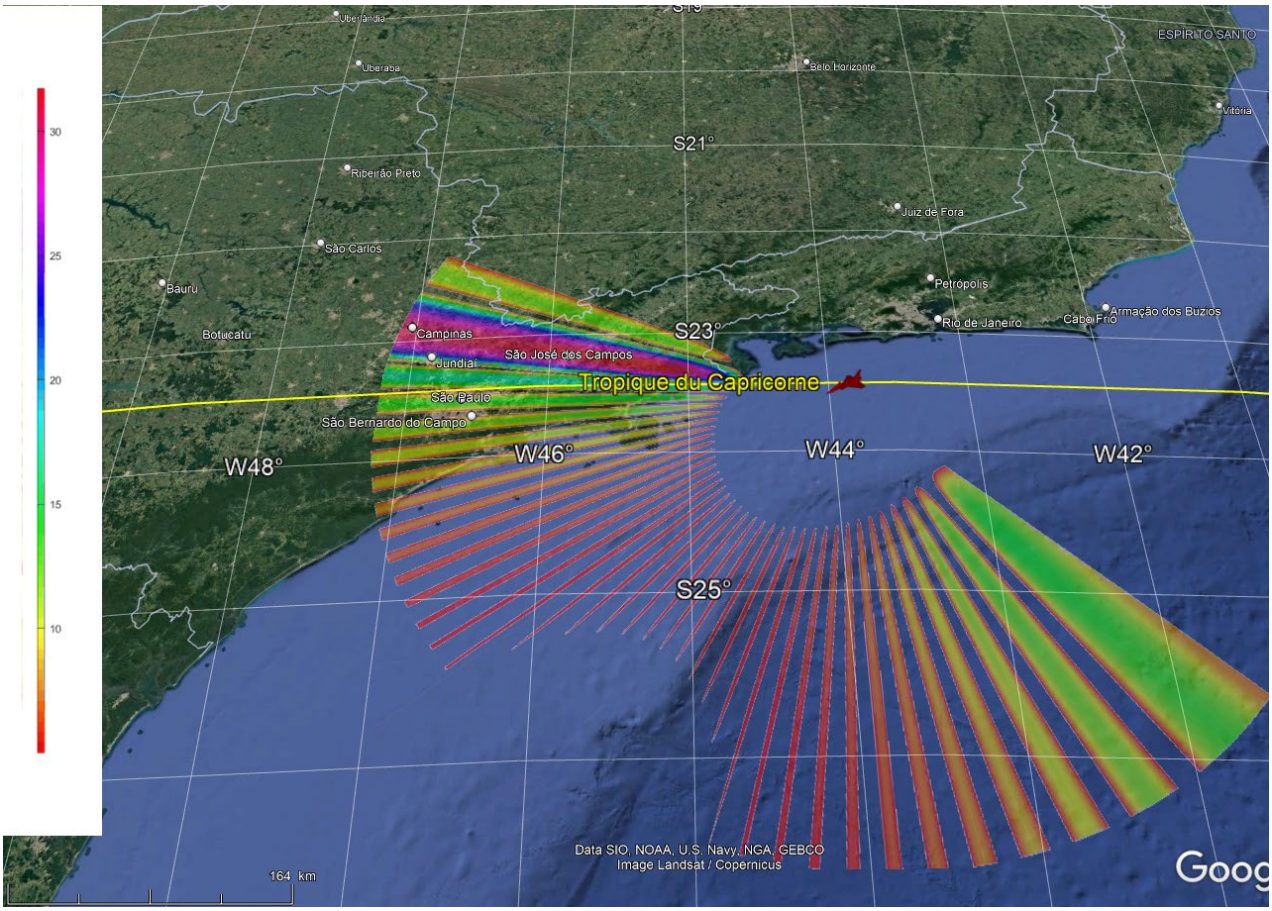

2.7.4.1.2 Deployment of IMT small cells Base Stations

As described in section 2.7.1.2.2, the methodology for deploying IMT hotspots using fixed population density thresholds is applied here. The population density threshold is computed with the publicly available data from NASA and hosted by the Columbia University[16]. Data collected as a set elementary tiles have a 0.008333° × 0.008333° (longitude, latitude) resolution, ensuring a 1km^2 accuracy level for the population density threshold assessment.

Due to the variability of the visibility area of the aircraft during its flight, the urban, suburban area as well as the number of IMT stations to be deployed for every environment also vary as depicted in the below pictures. The fact that the area size for urban environment exceeds 200 km^2 (around 600-700 km^2) as recommended by TG/5-1 is not a contradictory observation if it is recalled that the simulation area contains more than one dense urban city (Sao Paulo, Rio Janeiro…), resulting in multiplying the so-agreed "city structure: urban +suburban with full/partial built-up area city".

16 https://sedac.ciesin.columbia.edu/data/set/gpw-v4-population-density-rev11

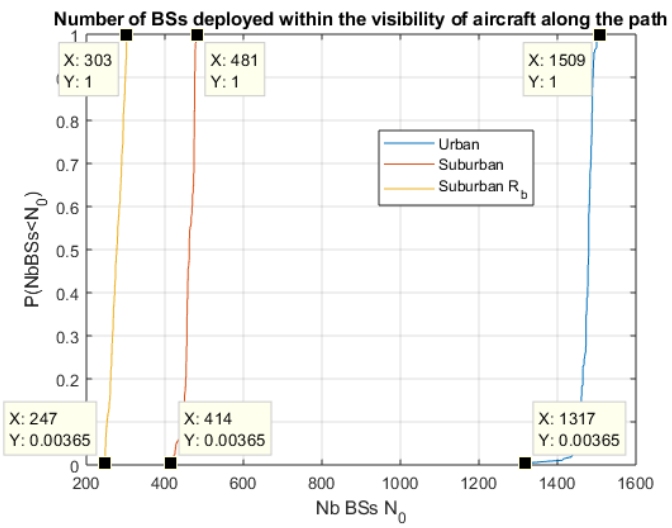

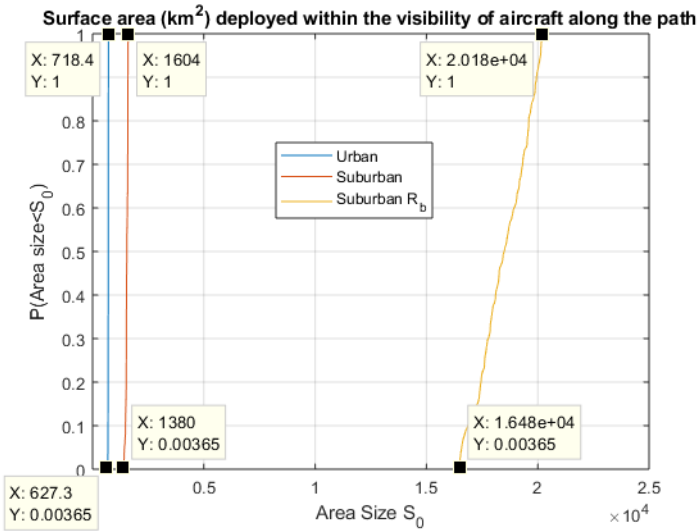

As expected, the surface of the suburban R_b environment is significantly bigger than for the other because the large range of retained population densities 100- 7000 compared to the other ones (7000-14500, >14500 inh/km^2). However, because of the R_b factor, the resulting number of BSs is smaller than for the other environments with full built-up areas.

Once urban and suburban (partially or fully built-up) elementary tiles are known, micro BSs can be randomly deployed in any of them, in accordance with the density of every environment.

Noting that the elementary tiles are very small (<1 km^2 size), there is no stake in distinguishing any deployment location over another one within the same tile: all micro BSs within the same tile can be processed (BS antenna gain computation) without the knowledge of the location since its angular orientation towards the airborne radar (φ, θ) only matters.

The spatial distribution of smallcells BSs looking angle towards the aircraft can be exhibited for two exemplary positions of the aircraft as follows:

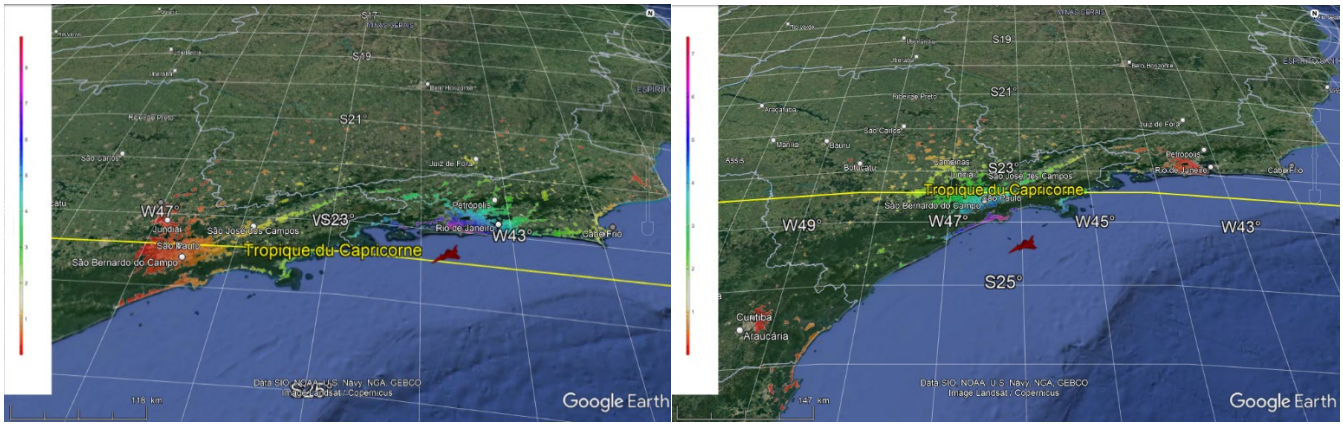

For any location of the aircraft within the path, the overall range of bearing angles from ground stations within the simulation area stands around 0-9°. It should also be noted that at any fixed ground location, the elevation angle (of the site) towards the aircraft varies with the position of the airborne receiver. For example, the left figure above corresponding to the start of the path shows around 7-8° inside Rio-Janeiro (purple colour) while the same location presents the lowest value 0-1° (red) when the aircraft flies close to Sao Paulo. In addition, if the bearing elevation angles are strictly lower than 10° and reminding that the main lobe of the BS hotspot is larger than 20° and that $\theta_{e-tilt} \geq -10°$ for more than

90% of the case, it is concluded that portion of IMT BSs whose azimuth positioning is roughly facing the aircraft would likely point their main lobe (in elevation) towards the aircraft.

Micro Bss are not necessarily oriented in the same azimuthal direction towards the aircraft, that's why the orientation of each BS antenna should be treated independently of the other ones. However, if Monte-Carlo simulations method is used to compute the aggregate interference, from the time perspective, a fixed azimuth positioning for every station φ_i (i being the index of micro BS antenna) should be considered at every run j (i.e. the orientation of a sector, if randomly generated at the first event should be kept the same for the other events i.e. $\forall(i_1, i_2, j), \varphi_{i_1,j} = \varphi_{i_1}$ and $\varphi_{i_1,j} = \varphi_{i_1} \neq \varphi_{i_2}$ in general). The idea of setting fixed positioning of any micro BS within the events does not apply for beam steering of the BS antenna. The mobility and diversity (a number of UEs to be simultaneously served by the BS) of the user terminal bring the BS antenna to time-varying[17] beam steering (in φ_{scan} and θ_{e-tilt}) with the events of the Monte-Carlo simulations.

2.7.4.1.3 Deployment of IMT User Equipment

For micro BS deployment, it is understood that UEs are assumed to be distributed using uniform (in coordinates (x,y), deployment. For the indoor/outdoor deployment, a spatial consistency in the generation of outdoor and indoor location is applied in order to ensure a relevance any indoor/outdoor locations among the run of the Monte-Carlo simulations i.e. by avoiding to set indoor and outdoor in the exact location[18]. Below pictures reflect the information related to the geographical distribution of user terminals (expressed as the *probability density function* of the distance between UE and BS and azimuth of positioning towards a reference direction).

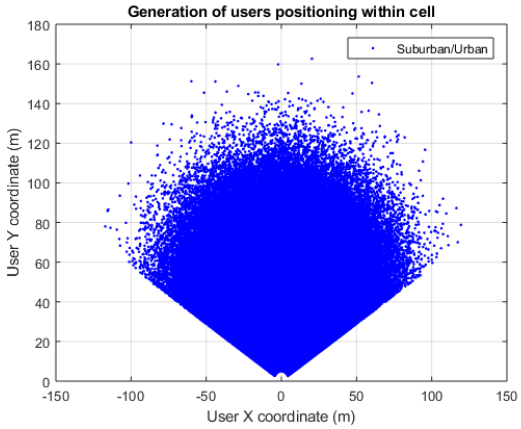

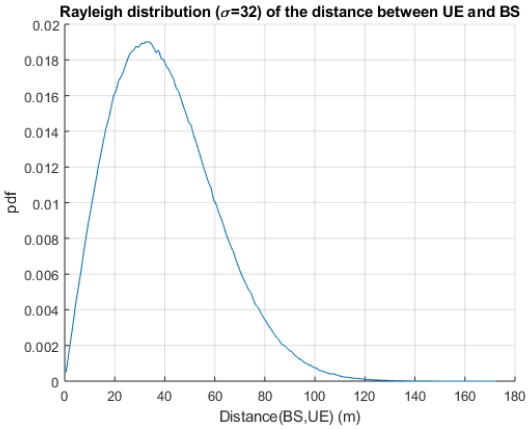

Transmission power is derived from coupling loss involving BS and UE antenna gains as well as pathloss calculation between UE and BS where it is noted that:

- Outdoor pathloss is computed using Report ITU-R M.2412 Urban micro Model B & Probability of *Line of Sight (LoS)*
- Outdoor-indoor penetration loss between BS and UE is computed also using Report ITU-R M.2412 while analytical formula and parameters values from Recommendation ITU-R P.2109-1 are used to determine the penetration loss between the transmitting terminal and the radar receiver for the interfering radio link.

[17] Except if the user is located close to the BS antenna. In such case, it will be covered by the sidelobes of the beam.

[18] Excluding the scarce case with indoor user becoming outdoor with door or window opened

This means that any radiated power of the terminal towards the aircraft (interfering link) differs from the radiated power towards the BS antenna (wanted link).

2.7.4.1.4 Impact of the IMT User Terminals in the sharing study

Similarly, to another study submitted by France (Doc. 5D/967) within the same frequency, band the aggregate interference from user terminals is assumed to be negligible towards the one from micro BSs and does not need to be carried in the analysis.

2.7.4.2 Monte-Carlo simulations approach

2.7.4.2.1 Calculation of the aggregate interference from IMT Base Stations

If the description of the airborne radar operation and the IMT BSs deployment have been previously provided in the previous section, it's important to put the emphasis on the orientation of the radar antenna towards the sources of interference as well as the operational characteristics of an airborne radar.

- Indeed, if the aggregate interference is calculated by mixing different orientations of the radar antenna (in particular when the antenna back-lobes face the sources of interference), the averaging effect from the integration of those data may lead to an underestimation of the impact over the radar in some directions (with active BSs). That's why it appears important to protect the performance of the radar[19] in every angular direction. Document 5D/1007 is a LS sent by WP 5B which gave such insight on how to handle the antenna of the radar for the frequencies range 3 100-3 400 MHz in particular that *for aggregated scenarios, WP 5B proposes WP 5D to take into account the interference received by the radar only when pointing in the direction of the IMT deployment.* Assuming that this guidance for the coexistence involving radiolocation systems is not specific to the targeted frequencies band, it's understood that similar approach can be taken for other frequencies allocated to the radiolocation as a primary service, for example in 10 000-10 500 MHz.
- During the 5D previous meeting, discussions driven by one input contribution (***5D/1183***) highlighted the need to **consider the technical and operational characteristics** of the radar system in any dynamic study dealing with interference affecting the receiver: *radar azimuth and elevation scanning* of the rotating antenna, complete radiation pattern (*Interference is received by the radar from the whole radar antenna pattern including the antenna mainlobe, sidelobes and back lobes*).

The two aforementioned points are not contradicting each other and can be covered together if the sharing study tackles a scenario with an aircraft in motion with a rotating antenna whose radiation pattern is fully modelled and for which every aggregate interference *sample represents a unique pointing direction of the radar antenna*[20] beam. This is precisely what was carried out in document ***5D/1191*** although this is relating to another Agenda Item (1.4).

That's why this study considers the aggregate effect of interference but with a spatial representation of the radar pointing angles for which the interference at the radar exceeds the I/N protection criterion.

---

[19] Expressed in terms of capability to detect and identify objects.

[20] See contribution 5D/1191 Section A4.7.1.5.1

For any given position of the aircraft antenna #k ($k \in [\![1, NbPositionsAircraft]\!]$), the simulation area (delimited by the antenna footprint of the aircraft in its visibility area) is set and micro BSs can be geographically deployed within. Afterwards, the computation of the aggregate interference can be performed as follows:

Step 1: Computes the BS antenna gain for every active small cell BS #*i* ($i \in [\![1, NbBSs^{21}]\!], Card(i) = NbActiveBSs^{22}$) at every event #*j* ($j \in [\![1, NbEvents]\!]$) towards the radiolocation radar. Each event relates to an IMT-2020 radio sub-frame period $T_{sub\text{-}frame\ IMT}$ for which one or several BSs are transmitting while $NbEvents$ is the number of IMT-2020 radio sub-frames within the time slot of radar T_{radar} for a process of the data collected per beam steering. The gain is respectively denoted $G_{BS\ u/sub}(\varphi_{i(j,k)}, \theta_{i(j,k)}, \varphi_{scan\ i(j,k),j}, \theta_{e-tilt\ i(j,k),j})$ for urban and suburban environments. The reason for distinguishing suburban from urban environment in this computation is artificial as their spatial distribution only differs. Reminding that active BSs are not necessarily the same for every event #*j* (short-term perspective with few tens, hundreds of *ms* difference) and more generally for different positions of the aircraft #*k* (long-term perspective with few seconds, minutes difference), the dependency of the active BS #*i* over the event #*j* and the position of the aircraft #*k* is reflected through the expression $i(j,k)$. Such expression is useful to depict the only spatial variation of every BS antenna positioning towards the airborne radar ($\varphi_{i(j,k)}, \theta_{i(j,k)}$) while beamforming angles ($\varphi_{scan}, \theta_{e-tilt}$) can also vary for the same BS antenna along the event #*j* (and also for a given location of the aircraft #*k*) because of different or varying in mobility served UE. Finally, one could notice that the antenna gain of every active BS located within the same tile is calculated at the same elevation angle towards the airborne receiver, but generally with different beam-steering and azimuth positioning.

Step 2: The clutter loss is computed for every active urban and suburban micro BS #*i* ($i \in [\![1, NbBSs^{23}]\!], Card(i) = NbActiveBSs^{24}$) at every event #*j* ($j \in [\![1, NbEvents]\!]$) towards the radar. This attenuation is respectively denoted $CL_{BS\ u/sub}(p_{i(j,k)}, \theta_{i(j,k)})$ for urban and suburban environments. Based on distribution of micro BSs elevation looking angles provided as examples in Section 2.7.4.1.2, the following distribution of attenuation related to these examples is exhibited for different environments (corresponding to 0-10° range) and clutter loss models.

---

[21] $NbBSs = NbUrbanBSs\ for\ BSs\ in\ urban\ areas, NBSs = NbSuburbanBSs\ for\ BSs\ in\ suburban\ areas$

[22] $NbActiveBSs = NbActiveUrbanBSs\ for\ BSs\ in\ urban\ areas, NbActiveBSs = NbActiveSuburbanBSs\ for\ BSs\ in\ suburban\ areas$

[23] $NbBSs = NbUrbanBSs\ for\ BSs\ in\ urban\ areas, NBSs = NbSuburbanBSs\ for\ BSs\ in\ suburban\ areas$

[24] $NbActiveBSs = NbActiveUrbanBSs$ for BSs in urban areas, $NbActiveBSs = NbActiveSuburbanBSs$ for BSs in suburban areas

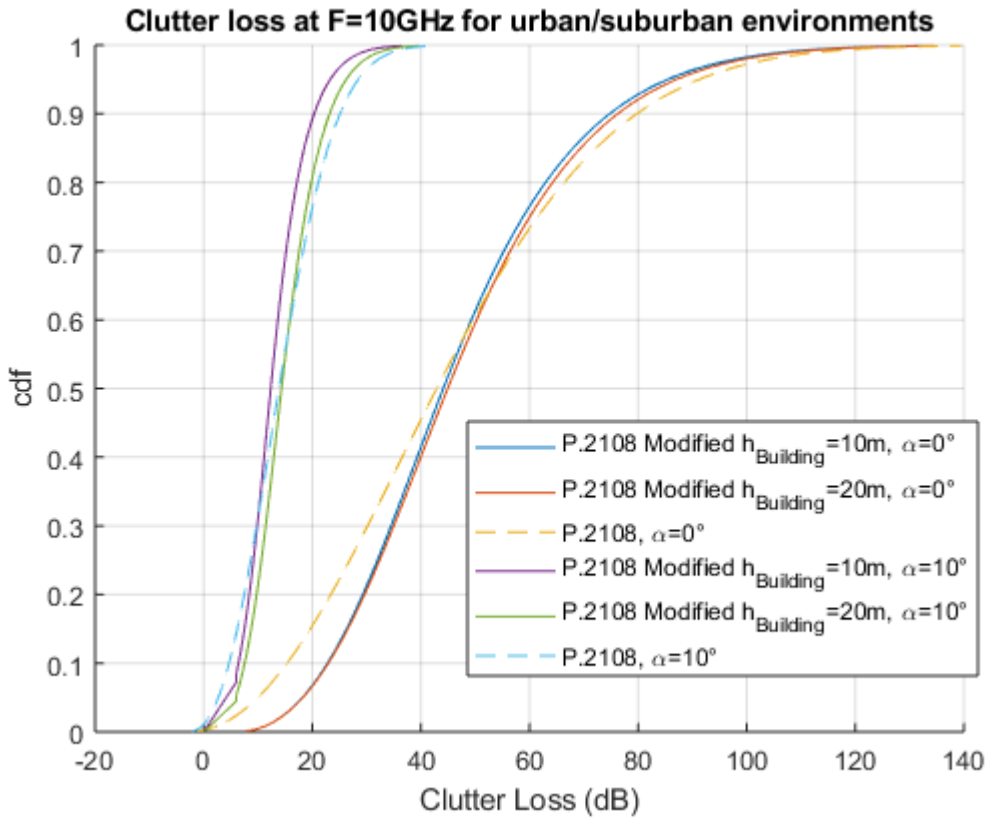

Step 3: The path loss (PL) between the airborne radar receiver and IMT stations are computed for every active small cell BS #i ($i \in [\![1, NbBSs^{25}]\!], Card(i) = NbActiveBSs^{26}$) at every event #$j$ ($j \in [\![1, NbEvents]\!]$) towards the airborne radar. These attenuations are respectively denoted $PL_u(d_{i(j,k)})$ and $PL_{sub}(d_i(j,k))$ for urban and suburban environments[27]. In practice, this parameter can be calculated for every tile once (prior to the first event) and the pathloss value related to the tile pertaining active BSs is associated to these actives BSs.

Step 4: For an airborne radar antenna beam pointing ($\varphi_{scan\ radar\ k}, \theta_{e-tilt\ radar\ k}$) at a given position #$k$, its gain towards an active micro BS antenna #i $G_{Rx}(\psi_i, \varphi_{scan\ radar\ k}, \theta_{e-tilt\ radar\ k})$ is computed by calculating the angular discrimination between the orientation of the radar antenna and the tile "hosting" the active BS ψ_i . In practice, $G_{Rx}(\psi_i, \varphi_{scan\ radar\ k}, \theta_{e-tilt\ radar\ k})$ can be calculated for every tile and the ones hosting active BSs are used for the sharing study.

Step 5: The interference from every IMT active micro BS station #i at every event #j, for a given positioning of the aircraft #k is then derived by combining the previous parameters as well as the conducted power of the emitter and the polarization loss (denoted *Pol* and assumed to be 3dB) as follows:

---

[25] $NbBSs = NbUrbanBSs$ for BSs in urban areas, $NBSs = NbSuburbanBSs$ for BSs in suburban areas

[26] $NbActiveBSs = NbActiveUrbanBSs$ for BSs in urban areas, $NbActiveBSs = NbActiveSuburbanBSs$ for BSs in suburban areas

[27] Note that any micro BS operating in the same tile is subject to the same FSL and GL even though one is urban and the other is suburban

$$I_{BSu/subi,j,k}(mW) = \frac{P_{composite\ BS} \times G_{BS\frac{u}{sub}}(\varphi_{i(j,k)}, \theta_{i(j,k)}, \varphi_{scan\ i(j,k),j}, \theta_{e-tilt\ i(j,k),j}) \times G_{Rx}(\psi_{i(j,k)}, \varphi_{scan\ radar\ k}, \theta_{e-tilt\ radar\ k})}{CL_{BS\ u/sub}(p_{i(j,k)}, \theta_{i(j,k)}) \times PL_{\ u/sub}(d_{i(j,k)}) \times Pol}$$

Step 6: The aggregate interference from active BSs at every event *#j* (for a given location of the aircraft *#k*) for a given positioning of the aircraft *#k* can be deduced from the previous step and accounting the TDD factor *TF* apportionment between BS and UE:

$$I_{agg,j,k} = \sum_{i(j,k)} I_{BSu\ i,j,k} + \sum_{i(j,k)} I_{BS\ sub\ i,j,k}$$

Step 7: The aggregate interference received by the airborne radar receiver is derived over a period of data processing T_{radar} and corresponds to the integration of the aggregate interference $I_{BS\ agg,j,k}$ previously computed for every event *#j* from the previous step and accounting the TDD factor *TF* apportionment between BS and UE:

$$I_{agg,k} = TF\left(\frac{1}{NbEvents}\sum_{j=1}^{NbEvents} I_{BS\ agg,j,k}\right) + (1-TF)\left(\frac{1}{NbEvents}\sum_{j=1}^{NbEvents} I_{UE\ agg,j,k}\right)$$

According to sub-section 4.1.3, the aggregate interference from UEs is negligible towards micro BSs, hence the aggregate interference is given as follows:

$$I_{agg,k} \approx TF\left(\frac{1}{NbEvents}\sum_{j=1}^{NbEvents} I_{BS\ agg,j,k}\right)$$

Noting that the sharing study deals with co-channel sharing between radiolocation and IMT, using interference-noise-to-ratio $I_{agg,k}/N$ as a metric does not require to use the radar receiving bandwidth. Consequently, the radar receiver noise power *N* and the aggregate interference $I_{agg,k}$ will be expressed per MHz. Hence, given the radar noise figure (6 dB), $N \approx -108\ dBm/MHz$. Noting that the beam-steering of the aircraft array $(\varphi_{scan\ radar\ k}, \theta_{e-tilt\ radar\ k})$ as well as the positioning of the aircraft (during its flight) are time dependent, no integration of $I_{agg,k}/N$ over the position of the aircraft *#k* is generally performed in order to identify angular directions of pointing (from the radar antenna) subject to exceedance of the protection criterion from the other. An exception will apply for any target tracking i.e. a scenario where a given beam-steering is maintained over some consecutive locations of the aircraft.

2.7.4.2.2 Analysis of the results

2.7.4.2.2.1 Scanning mode of the radar

For every position of the aircraft along the path, the airborne radar is scanning to a given direction $(\varphi_{scan\ radar\ k}, \theta_{e-tilt\ radar\ k})$ for a T_{radar} seconds duration and the aggregate interference during that period is assessed through Monte-Carlo simulations. A mean of the aggregate interference from every IMT-2020 sub-frame $T_{sub\text{-}frame\ IMT}$ over the time integration of a received radar pulses signal T_{radar} needed to perform the detection of any object within the given angular direction (for one elementary solid angle pointed by the radar antenna beam). The averaging process is done for $T_{radar}/T_{sub\text{-}frame\ IMT}$=*200ms/1ms*=200 samples. Resulting mean I_{agg}/N[28] is generated over every position of the aircraft and a plot along the path of the airborne receiver for two different assumptions of clutter

[28] where I_{agg} relates to the aggregate interference and N the noise level received by the radar antenna.

loss model (using Rec. ITU-R P.2108, Annex 1 Doc. 3K-3M/178) and different pathloss model (Free-Space-Loss Recs. ITU-R P.525, ITU-R P.528-5 with time percentage t=5% and 10%) where the protection criterion (I_{agg}/n=-6dB) is reflected through a green horizontal line. The results for clutter loss model from Doc. 3K-3M/178 only is provided in the below figure for the sake of readability.

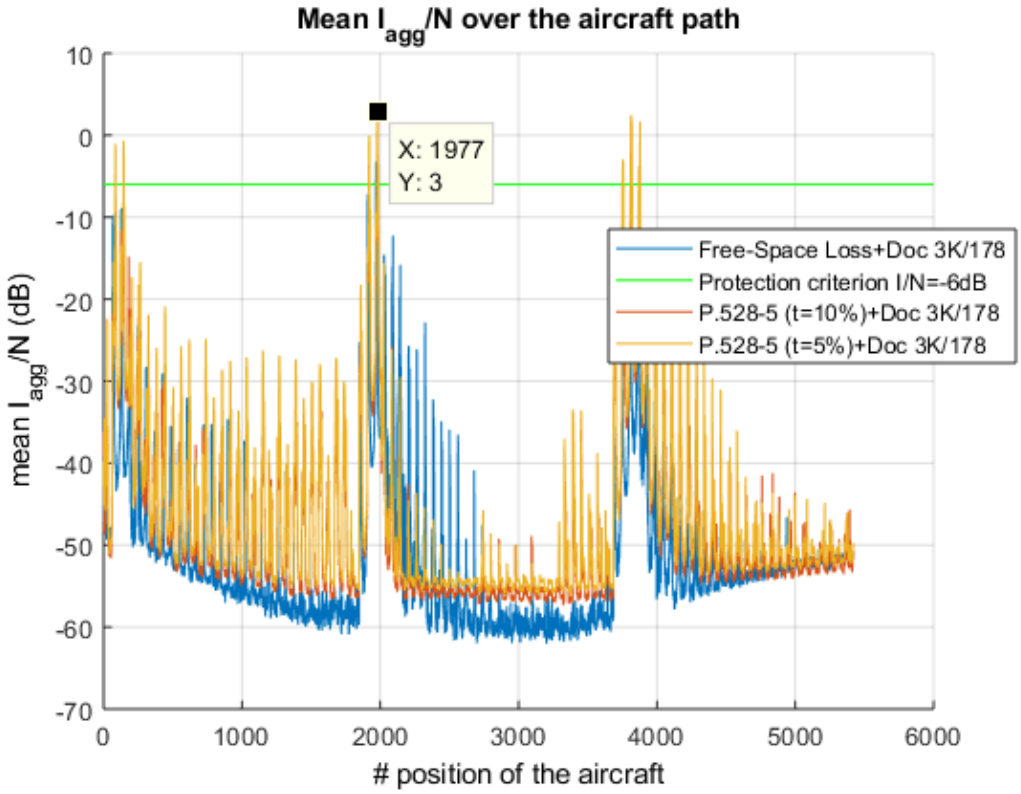

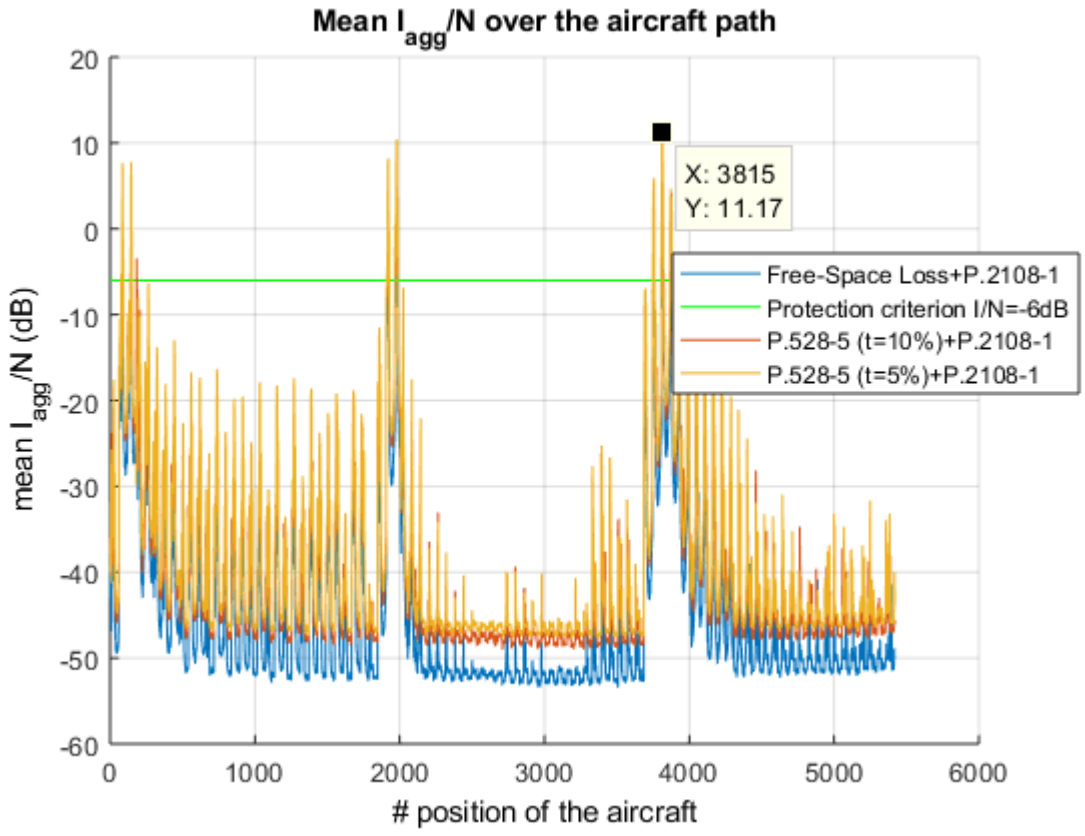

From these scenarios, several observations are of interest:

- Any point of every curve is the result of an averaging of 200 successive $(I_{agg}/N)_k$ samples[29], $k \in [\![1,200]\!]$, each sample coming from a different IMT-2020 sub-frame. Each point reflects the received aggregate interference for a given position of the aircraft suggests that aggregate interference samples have values below or above that mean.
- Strong variations of the mean I_{agg}/N (-60..3[30] dB) in the chronogram express the transient nature of this dynamic study: scanning effect of the radar antenna beam (covering with main lobe/sidelobes/back-lobes the ground location of IMT deployment) as well as the mobility of the aircraft (distance from the sources of interference) during its mission.
- For all scenarios (different clutter loss models/different propagation models), there are always several moments during which the exceedance of the protection criterion (I_{agg}/N=-6dB) is observed and there is a risk that the radar to be blinded during that period. More specifically, there are three (non-continuous) periods of exceedance in the chronogram: position #85-147, #1917-1985 and #3752-3879. The difference in the results for those use cases arises from the number of events for which an exceedance of the protection criterion is met as well the exceedance level (0-9 dB when using P.528-5 with *t=5%*+Clutter loss model from Doc 3K/178, 0-17 dB using P.528-5 with *t=5%*+P.2108). Although it is not surprising that aggregate interference can be higher when assuming P.528 with lower percentage of time, the fact that for few positions of the aircraft the mean I_{agg}/N is lower for these cases is due to the fact that results were not obtained for the same samples of the Monte-Carlo simulations[31]. Moreover, it is worth mentioning that these events of interference generally come by packet (from 2 to 10 for this case) of scanned directions and not on an isolated perspective. This means that the radar receiver could not properly operate over a block of consecutive angular directions i.e. could miss targets detection or result in false alarm. Noting that these scanning angles are 2° resolution (in both elevation and azimuth) for the study, this means that up-to 20° in the horizon of scanned angles from the airborne receiver could not be correctly processed and led to erroneous information (no possibility to detect any object of interest within this spatial area). The following picture gathers the angular directions for which the aggregate interference exceeds the protection threshold for one scenario (ITU-R Rec P.528-5 with t=10% and using Clutter loss model from Doc 3K/178). These events are depicted through yellow spots.

[29] $(I_{agg}/N)_k$ being generated at $[(k-1)T_{sub-frame\ IMT}, kT_{sub-frame\ IMT}]$ $interval$,

[30] 3dB is achieved when using ITU-R Rec P.2108-1 model (and Rec P.528-5 with t=5%) to compute the attenuation due to clutter

[31] For two different propagations models (e.g. P.525 and P.528 with t=10%), the aggregate interference from IMT hotspots were generated through two Monte-Carlo simulations and not the same one.

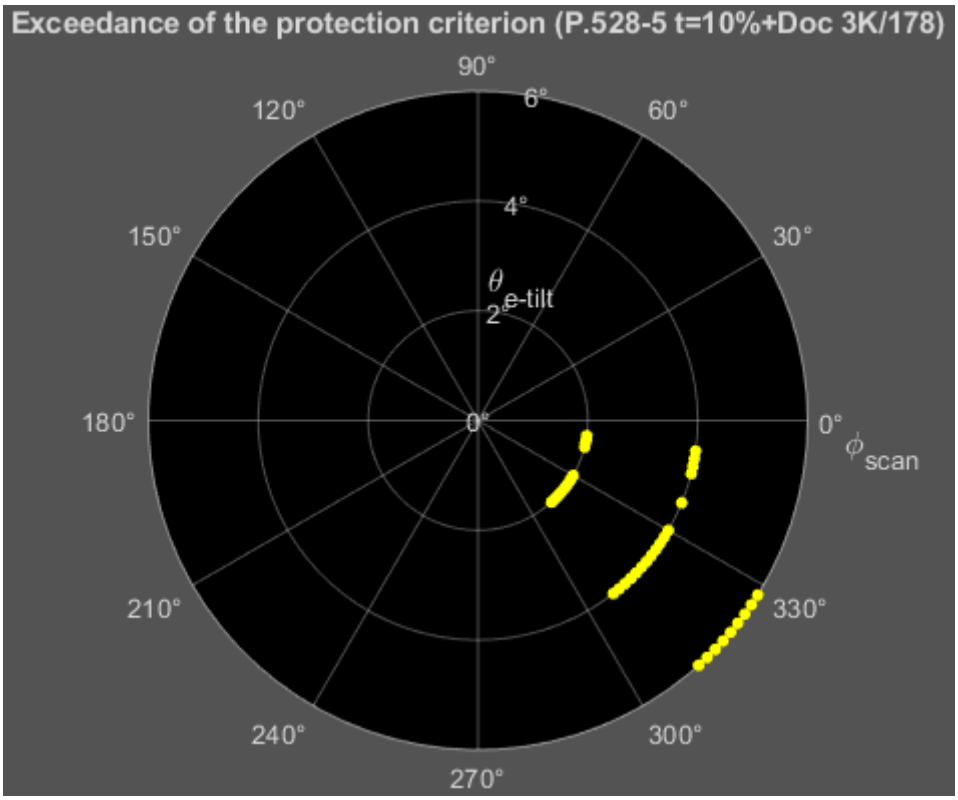

The second bullet raises the crucial question of the duration of such exceedance: one could claim that because of the rotation of the radar antenna (mechanical or electronical beam), it's always possible for the radar to tolerate a short event of exceedance from the moment when it loops again the direction subject to interference (criterion) exceedance, the interference was transient and has been already vanished. That statement is partially true for *Track While Scan* radiolocation systems (which is particularly the case for electronic scanned phased-array radar) when the targets are the angles for which the radar was potentially blinded or provided a false alarm/missed a target. The system under consideration for this study (A12) is able to perform both search (scanning angles) and tracking because it performs digital beamforming with multiple beams for multiple purposes.

2.7.4.2.2.2 Tracking mode of the radar

As suggested in the previous section, it is important to investigate how long the exceedance of the protection criterion lasts for every angle subject to that interference event. This means that *TWS* process will be simulated by maintaining a given pointing angle if the I_{agg}/N is above the threshold during the flight of the radar. Such focus will last while the protection criterion is exceeded at this angular direction of the radar antenna. In light of the numerous scenarios considered for the case where the aircraft is scanning the horizon during the flight (6 with different propagation and clutter loss models) and the number of events with an exceedance of the protection criterion, it is proposed to consider few different cases such as high range and isolated scanned angles subject to the interference threshold exceedance to perform a track of these angular directions. The propagation conditions for the tracking angles analysis in this sub-section are ITU-R P.528-5 with t=10% for the pathloss and the clutter loss model comes from Doc 3K/178.

The first case to be addressed relates to a single position of the aircraft (#1985T_0 where T_0=200ms[32]) where the protection criterion is exceeded, corresponding to $(\varphi_{scan\ radar}, \theta_{e-tilt\ radar}) = (-22°, 4°)$ depicted in red point in the below picture.

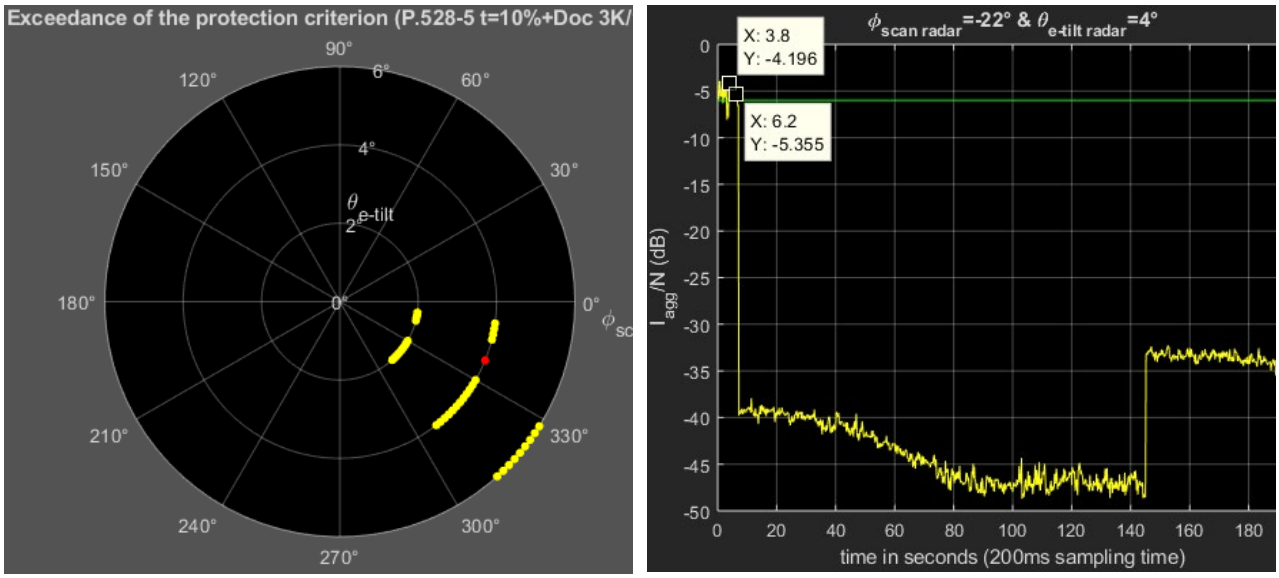

A tracking of this angular direction is performed by the radar over for more than 3 minutes (200s) during the operation of the aircraft (while scanning other directions) and the resulting I_{agg}/N is computed at every time snapshot (200ms) in the right side above figure. The yellow curve shows a short period (t_1-t_0=6.2-3.8<3s) where the protection criterion is slightly exceeded probably because the aircraft is moving and the IMT hotspots aren't . Afterwards, the aggregate interference falls down in -40..-50 dB and increases (but without exceeding the protection criterion). This drastic variation in time of I_{agg}/N likely can be explained by noticing that although sources of interference populate the coast over a long distance, those that have had a dominant effect are going further from the aircraft.

The second case relates to successive positions of the aircraft (between t=3810T_0 and t=3819T_0 where T_0=200ms[33]) corresponding to consecutive pointing angles: $(\varphi_{scan\ radar}, \theta_{e-tilt\ radar}) = (-34..-52°, 4°)$.

[32] Belonging to the 2nd period of exceedance of the protection criterion as previous described in bullet #3

[33] Belonging to the 3rd period of exceedance of the protection criterion as previous described in bullet #3

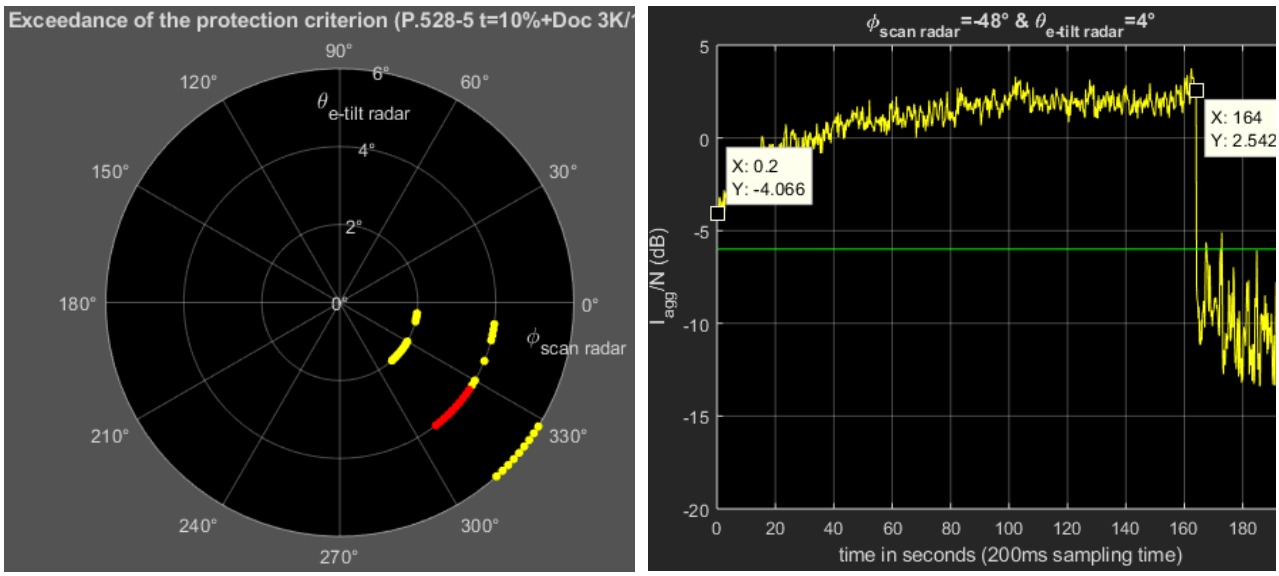

Curve related to one pointing angle is depicted as an example in above right-side figure. The exceedance of the protection criterion occurs for more than 82% of the time slots with more than 2 continuous minutes (t_1-t_0=164-0.2>120s) and higher level of exceedance of the protection criterion (up-to 2.5dB). When looking at the I_{agg}/N value at t=0s (around 2dB above the protection criterion) for the same example, it's worth noticing that the duration of the interference exceedance could have been higher if this pointing angle $(\varphi_{scan\ radar}, \theta_{e-tilt}) = (-48°, 4°)$ was scanned before the aircraft position it has been considered for the study (to decrease monotonically below -6dB). All pointing angles subject to tracking process were triggered over for the same duration (according to abscissa axis) but at different (close) instants in order to be compliant with instant of scanning angle of the airborne radar. Statistics on the "interfered time-slots' are provided hereafter:

TABLE 10

Statistical occupancy of the interfered radar time-slot at $\theta_{e-tilt\ radar}$=4°

Pointing $\varphi_{scan\ radar}$ angles	**-52°**	**-50°**	**-48°**	**-46°**	**-44°**	**-42°**	**-40°**	**-38°**	**-36°**	**-34°**
ratio of time-slots exceeding the protection criterion	77.7%	79.2%	82.0%	81.4%	81.2%	81.0%	80.8%	76.5%	65.5%	53.2%
Max continuous duration of the interference excess	139.6s	149.4s	163.8s	163.4s	163.0s	162.6s	162.2s	141.8s	123.4	100.8s

From the above table, it can be seen that for $\boldsymbol{\varphi_{scan\ radar}}$ values ranging -52° to -36°, the interference exceedance would last at least 2 minute (≥123.2s) and more than 1 minutes over 18° azimuthal angular sector. Thus, this case is even more critical than the previous one in the sense that the radar might lack correct information (missing objects, false alarm) for a large angular cone of scanning for a long period of time (more than 1 minute) for a given elevation angle (4°).

The impact of the analysis carrying out the aggregate interference during a tracking process cannot be stated as a worst-case scenario

- As it aims at accounting the rotating nature of the antenna as well as the mobility of the aircraft and not intentionally pointing to the direction of sources of interference. A practical situation was considered with a dynamic analysis where an aircraft operates outside territorial waters with a scanning radar and a track function if an area/direction of interest is to be initiated by the pilot. The fact that a pointing angle suffers from the exceedance of the protection criterion is one reason for performing a tracking within that direction in order to ensure the radar is still able to detect objects within that direction.
- As a lower percentage of time (t=5%) for ITU-R Rec P.528-5 was not considered to compute the pathloss, as well as clutter loss model using ITU-R Rec P.2108-0 which would have led to an overall lower attenuation. These other assumptions would probably result in larger range of continuous pointing angles subject to potential interference above the protection threshold.
- The antenna pattern of the aircraft was computed in compliance with real systems embedded on French aircraft and considered the lower peak value for airborne radar system A12 (36 dBi) from ITU-R Rec M.1793 compared to the higher peak value taken in most other studies (42 dBi). Although the 3dB beamwidth is a little larger for this pattern than for 42 dBi, the difference in the number of IMT hotspots within 3dB contour from these two antenna footprints is far from compensating the seven dBs difference between those two peak gains.

These compatibility results established within an urban/suburban area covered by the airborne radar antenna when surrounding the coastlines can be generalized to other use cases without affecting the geometry of the interference scenario. For instance, similar conclusions would be drawn if the aircraft operates far from the coastlines and is approaching the territorial waters.
A way to reduce the duration of the exceedance of the protection criterion (or to remove the exceedance) would be to mitigate the *Total Radiated Power* of IMT hotspots in order to ensure the aggregate interference hardly exceeds the protection threshold. A 8 dB reduction of the TRP would enable to limit the occurrence of the interference to isolated angular direction (and not an angular sector) for few seconds (5-6s) under the considered scenario. If a more conservative scenario was considered (with P.2108 clutter loss model or/and lower percentage of time t=5% for P.528), the TRP reduction would be much bigger

2.7.4.3 Summary and conclusion

This contribution aimed at analysing the aggregate interference received by an airborne radar in motion and operating from IMT-2020 micro BSs deployment in 10-10.5 GHz. The aircraft was assumed to fly along the coast at 9 000 m (above the mean sea level) with an electronic scanned phased array whose beam steering varies. This means that its main lobe, side lobes, back-lobes can be directed towards the location of the IMT network when looping the landscape in accordance with the operation of a radar assumed to steer the beam continuously in different directions. The fact that aggregation interference is assessed per pointing angle of the aircraft antenna array and not by integrating the interference over different scanning angles ensures that the consistency between the protection of the airborne receiver and its performance (objects detection over different directions). Such approach is in accordance with the guidance from WP 5B LS (5D/1007) in particular that *for aggregated scenarios, WP 5B proposes WP 5D to take into account the interference received by the radar only when pointing in the direction of the IMT deployment.*

The study was divided into two parts:

- The scanning phase where two clutter loss models were used in the simulations (Rec. ITU-R P.2108-1 for the slant path and a mathematical model from Annex 1 of Document 3K/178 under evaluation by a Correspondence Group designed by WP3K/3M) and two propagation models (Free Space Loss and Rec P.528-5) for the scanning analysis. Results showed that for any clutter loss, propagation model scenarios, there is always a risk for the radar to be affected from interference within a range of consecutive azimuth/elevation pointing angles, resulting in false alarm/missed target detection in several angular sectors.
- The tracking phase for some beam pointings where the protection criterion was exceeded. A set of assumptions from the scanning phase was further investigated[34]. It was observed that the aggregate interference above the protection threshold for several pointing angles of the aircraft antenna can be up-to I_{agg}/N=1.5 dB and can last several minutes.

Since the aggregate interference is dominated by the main lobe of the BS hotspots, the application of *Sidelobe Suppression Levels (SSL)* to the radiation pattern of IMT-2020 stations would not mitigate the in-band emissions from micro BSs. The coexistence between Radiolocation and IMT-2020 hotspots at 10-10.5 GHz is difficult and would require at least 8dB in-band reduction of the *Total Radiated Power (TRP)* to hotspots to turn the aggregate interference into transient events (i.e. occurring less than 1s) so that the airborne radar is capable to operate properly within the international areas while handling any transient exceedance of the interference threshold in specific single angular scanning direction from IMT stations located along the coastlines.

[34] ITU-R Rec P.528-5 with t=10%